



**HAL**  
open science

## Glacial cold-water coral growth in the Gulf of Cádiz: Implications of increased palaeo-productivity

Claudia Wienberg, Norbert Frank, Kenneth Mertens, Jan-Berend Stuut,  
Margarita Marchant, Jan Fietzke, Furu Mienis, Dierk Hebbeln

### ► To cite this version:

Claudia Wienberg, Norbert Frank, Kenneth Mertens, Jan-Berend Stuut, Margarita Marchant, et al..  
Glacial cold-water coral growth in the Gulf of Cádiz: Implications of increased palaeo-productivity.  
Earth and Planetary Science Letters, 2010, 298 (3-4), pp.405-416. 10.1016/j.epsl.2010.08.017 . hal-02890246

**HAL Id: hal-02890246**

**<https://hal.science/hal-02890246>**

Submitted on 24 Jun 2021

**HAL** is a multi-disciplinary open access archive for the deposit and dissemination of scientific research documents, whether they are published or not. The documents may come from teaching and research institutions in France or abroad, or from public or private research centers.

L'archive ouverte pluridisciplinaire **HAL**, est destinée au dépôt et à la diffusion de documents scientifiques de niveau recherche, publiés ou non, émanant des établissements d'enseignement et de recherche français ou étrangers, des laboratoires publics ou privés.

# Glacial cold-water coral growth in the Gulf of Cádiz: Implications of increased palaeo-productivity

Claudia Wienberg<sup>a,\*</sup>, Norbert Frank<sup>b</sup>, Kenneth N. Mertens<sup>c</sup>, Jan-Berend Stuut<sup>d,a</sup>,  
Margarita Marchant<sup>e</sup>, Jan Fietzke<sup>f</sup>, Furu Mienis<sup>a,d</sup>, Dierk Hebbeln<sup>a</sup>

<sup>a</sup> Center for Marine Environmental Sciences (MARUM), University of Bremen, Leobener Str., 28359 Bremen, Germany

<sup>b</sup> Laboratoire des Sciences du Climat et de l'Environnement (LSCE), Bât.12, Avenue de la Terrasse, F-91198 Gif-sur-Yvette, France

<sup>c</sup> Research Unit Palaeontology (RUP), Ghent University, Krijgslaan 281 S8, 9000 Ghent, Belgium

<sup>d</sup> Royal Netherlands Institute for Sea Research (NIOZ), Landsdiep 4, 1797 SZ t'Horntje (Texel), The Netherlands

<sup>e</sup> Departamento de Zoología, Facultad de Ciencias Naturales y Oceanográficas, Universidad de Concepción, Casilla 160-C, Concepción, Chile

<sup>f</sup> Leibniz-Institute of Marine Sciences, IFM-GEOMAR, Wischhofstr. 1-3, 24148 Kiel, Germany

\* Corresponding author. Tel: +49 421 21865652; Fax: +49 421 2189865652  
E-mail address: cwberg@marum.de (C. Wienberg)

1    **ABSTRACT**

2    A set of 40 Uranium-series datings obtained on the reef-forming scleractinian cold-water  
3    corals *Lophelia pertusa* and *Madrepora oculata* revealed that during the past 400 kyr their  
4    occurrence in the Gulf of Cádiz (GoC) was almost exclusively restricted to glacial periods.  
5    This result strengthens the outcomes of former studies that coral growth in the temperate  
6    NE Atlantic encompassing the French, Iberian and Moroccan margins dominated during  
7    glacial periods, whereas in the higher latitudes (Irish and Norwegian margins) extended  
8    coral growth prevailed during interglacial periods. Thus it appears that the biogeographical  
9    limits for sustained cold-water coral growth along the NE Atlantic margin are strongly  
10   related to climate change. By focussing on the last glacial-interglacial cycle, this study shows  
11   that palaeo-productivity was increased during the last glacial. This was likely driven by the  
12   fertilisation effect of an increased input of aeolian dust and locally intensified upwelling.  
13   After the Younger Dryas cold event, the input of aeolian dust and productivity significantly  
14   decreased concurrent with an increase in water temperatures in the GoC. This primarily  
15   resulted in reduced food availability and caused a widespread demise of the formerly  
16   thriving coral ecosystems. Moreover, these climate induced changes most likely caused a  
17   latitudinal shift of areas with optimum coral growth conditions towards the northern NE  
18   Atlantic where more suitable environmental conditions established with the onset of the  
19   Holocene.

20

21   **Keywords:** cold-water corals; last glacial; productivity; aeolian dust; Gulf of Cádiz; NE Atlantic

22

23    **1. Introduction**

24    Along the NE Atlantic margin cold-water corals occur in a belt that extends from northern  
25    Norway (Barents Sea, 70°N; Lindberg et al., 2007) down to NW Africa (off Mauritania, 16°N;  
26    Colman et al., 2005). These ecosystems vary strongly with respect to their appearance,

27 structure and coral vitality. Large flourishing *Lophelia*-reefs occur along the Norwegian  
28 margin. With a horizontal dimension of several hundred meters to kilometres they  
29 developed to the largest known living cold-water coral reefs worldwide (Fosså et al., 2005).  
30 Along the Irish margin cold-water corals are associated with coral mounds that vary in  
31 height from a few metres up to 380 m being often densely covered by living coral colonies  
32 (Wheeler et al., 2007, and refs. therein). Further to the south, cold-water corals mainly  
33 occur as isolated colonies or accumulations of fossil corals in the Bay of Biscay (Reveillaud  
34 et al., 2008), on seamounts (Duineveld et al., 2004) and within canyons along the Iberian  
35 margin (Tyler et al., 2009), and on coral mounds along the NW African margin (Wienberg et  
36 al., 2009).

37

38 Along with the geographic distribution, a distinct stratigraphic pattern regarding the  
39 development of cold-water coral ecosystems along the NE Atlantic margin has been  
40 observed during the last glacial-interglacial cycle. Reefs of Holocene age on the Norwegian  
41 shelf started to develop after the retreat of glaciers at the termination of the last glacial  
42 (Freiwald et al., 2004). The Irish coral mounds seem to be restricted to interglacials with a  
43 very few exceptions (Dorschel et al., 2005; Eisele et al., 2008) and the latest re-  
44 establishment of cold-water coral ecosystems appears to have been started after the  
45 Younger Dryas (YD) cold reversal (Frank et al., 2009). To the south along the French, Iberian  
46 and Moroccan margins, corals are suggested to have been widely distributed during the last  
47 glacial (Schröder-Ritzrau et al., 2005; Wienberg et al., 2009). In actual fact, although the  
48 Gulf of Cádiz (GoC) was recently identified to be an important cold-water coral site in the  
49 temperate NE Atlantic, this area is at present mainly characterised by so-called 'coral  
50 graveyards' with only very few living corals (Foubert et al., 2008; Wienberg et al., 2009).  
51 Such current depauperation of live coral ecosystems might be explained by the recent  
52 warm and oligotrophic conditions in the GoC forcing reduced food availability (Wienberg et  
53 al., 2009). In addition, tidal currents and internal waves that have been identified to be

54 important hydrodynamic processes for supplying food particles to and through the coral  
55 thickets (White et al., 2005; White et al., 2007) nowadays do not seem to play a major role  
56 in the GoC (Wienberg et al., 2009). However, the widespread occurrence of fossil corals  
57 suggests more favourable oceanographic conditions in the past. Indeed, initial datings  
58 revealed that cold-water corals have been common in the GoC during the last glacial  
59 (Wienberg et al., 2009).

60

61 The present study aims to refine and extend this observed stratigraphic pattern of coral  
62 occurrence along the NE Atlantic margin by 40 Uranium-series datings of reef-forming  
63 scleractinian cold-water corals from sediment cores retrieved in various areas of the GoC.  
64 Moreover, it is intended to relate the prosperity and/or demise of cold-water corals in the GoC  
65 to a distinct environmental and oceanographic setting that altered along with climate change.  
66 Thus, we aim to identify the main forcing factors triggering the development of cold-water coral  
67 ecosystems in the GoC.

68

## 69 **2. Regional setting**

70 The GoC is situated west of the Strait of Gibraltar, and thus connects the open North Atlantic  
71 Ocean and the Mediterranean Sea (Fig. 1). It is bordered by the Iberian Peninsula and the NW  
72 African coasts and extends from Cape St. Vincent at the southwestern tip of Portugal down to  
73 the Moroccan Atlantic margin at 33°N (Mauritzen et al., 2001). The Iberian continental shelf  
74 widens from ~15 km west of Faro to ~50 km further to the east (Garcia-Lafuente and Ruiz,  
75 2007), which is similar to the width of the Moroccan shelf (<60 km; Mittelstaedt, 1991).

76

77 The deeper basin of the GoC is characterised by a widespread occurrence of diapiric ridges  
78 and mud volcanoes (Somoza et al., 2003). Many of these mud volcanoes were identified to  
79 be covered by fossil cold-water corals (Somoza et al., 2003; Wienberg et al., 2009). Further  
80 conspicuous topographic features in the GoC are hundreds of coral mounds that are 20-30

81 m in height, and 50-200 m in length, and that are covered by fossil corals. They are  
82 restricted to the Moroccan margin where they have been found in a water depth between  
83 400 and 960 m (Foubert et al., 2008; Hebbeln et al., 2008; Wienberg et al., 2009). The coral  
84 mounds are mainly arranged as clusters and are situated amidst mud volcanoes and on top  
85 of diapiric ridges. Detailed knowledge about their origin, composition, and temporal  
86 development is to date still lacking.

87

88 Present-day oceanographic circulation in the GoC is dominated by the exchange of water  
89 masses between the Atlantic Ocean and the Mediterranean Sea (Ochoa and Bray, 1991).  
90 The relatively cold Atlantic Inflow Water flows eastward along the Iberian margin partly  
91 entering the Mediterranean Sea. It is composed of North Atlantic Surficial Water and North  
92 Atlantic Central Water (NACW). The upper-thermocline NACW deepens from about 300 m  
93 water depth close to the Strait of Gibraltar to about 600 m in the outer and southern parts  
94 of the gulf (Ochoa and Bray, 1991; Mauritzen et al., 2001). Below this level occurs  
95 Mediterranean Outflow Water (MOW). Flowing westwards through the Strait of Gibraltar,  
96 the MOW prevails in the northern gulf where it flows between ~500 and 1 400 m water  
97 depth above the North Atlantic Deep Water (NADW) (Ambar et al., 1999; Baringer and  
98 Price, 1999) and acts as a strong contour current (García et al., 2009). It is characterised by  
99 a permanent salinity maximum of ~36-37 and temperatures of 10.5 to 12°C (Fusco et al.,  
100 2008). For the southern GoC along the Moroccan Atlantic margin information about its  
101 hydrography is basically lacking (Machín et al., 2006). However, Pelegrí et al. (2005) suggests  
102 the presence of MOW at 800 m. This assumption is supported by the presence of an  
103 anticyclone or meddy close to the Moroccan shelf which implies at least some temporary  
104 southward transport of MOW along the Moroccan margin (Carton et al., 2002).

105

106 Today, the GoC constitutes an oligotrophic system with diminished primary production in  
107 the surface waters (Behrenfeld et al., 2005). Cold and productive upwelling is restricted to a

108 narrow band along the Portuguese coast (Garcia-Lafuente and Ruiz, 2007), and to the NW  
109 African margin south of 31°N (Cape Ghir) (Mittelstaedt, 1991; Pelegrí et al., 2005). Due to a  
110 prevailing anticyclonic circulation (Pelegrí et al., 2005), the basin of the GoC separates the  
111 Iberian upwelling from the upwelling off NW Africa (Garcia-Lafuente and Ruiz, 2007).

112

### 113 **3. Material and methods**

#### 114 **3.1 Core locations**

115 During three expeditions between 2003 and 2006, a set of ten coral-bearing sediment cores  
116 was collected from various sites in the GoC (Table 1). The coring sites comprise two mud  
117 volcanoes (Hespérides and Faro) along the Spanish margin and coral mounds along the  
118 Moroccan margin which are situated on top of the prominent Renard Ridge and its  
119 easternmost extension, the Pen Duick Escarpment. Finally, the southernmost core was  
120 collected north of Meknes mud volcano (Fig. 1).

121

122 The sediment cores have a length between 2.2 m and 8.6 m and are made up of abundant  
123 cold-water coral fragments embedded in a hemipelagic sediment matrix (Table 1). The  
124 sediment cores collected from mud volcanoes along the Spanish margin only contain cold-  
125 water corals in their upper parts, whereas the cores retrieved from coral mounds along the  
126 Moroccan margin are characterised by the occurrence of coral fragments throughout the  
127 sedimentary record.

128

129 To reconstruct oceanographic and environmental changes in the GoC during the last glacial-  
130 interglacial cycle and to compare this with the temporal distribution pattern of cold-water  
131 corals, sediment core GeoB 9064 (35°24.91'N, 06°50.72'W, 702 m water depth) was  
132 selected for a multiproxy study (Fig. 1). Core GeoB 9064 was collected along the Moroccan

133 margin (RV *Sonne* cruise SO175) and has a total length of 5.4 m. Samples for the various  
134 analyses were taken in 5-cm-intervals.

135

### 136 **3.2 U/Th age determination on coral fragments**

137 Forty fragments of the reef-forming scleractinian coral species *Madrepora oculata* and  
138 *Lophelia pertusa* were sampled at different core depths from the sediment cores listed in  
139 Table 1. Uranium-series measurements were performed using multi-collector ICP and  
140 thermo-ionization mass spectrometry at IFM-GEOMAR (Kiel, Germany; Fietzke et al., 2005)  
141 and at LSCE (Gif-sur-Yvette, France; Frank et al., 2004; Douville et al., 2010). Prior to  
142 analyses, samples were carefully cleaned to remove contaminants from the fossil skeleton  
143 surfaces according to procedures described by Fietzke et al. (2005) and Frank et al. (2004).  
144 Isotope concentrations and ratios as well as the absolute dates on the cold-water corals are  
145 provided in Table 2. Whole procedure blank values of this sample set were measured to be  
146 around 2 pg for thorium (Th) and between 4 and 8 pg for uranium (U). Both values are  
147 negligible compared to U- and Th-concentrations of the studied corals. The reproducibility  
148 of mass spectrometric measurements was tested using international U standard materials  
149 such as HU1 and NBL112, which provided identical values as the ones published by Fietzke  
150 et al. (2005) and Frank et al. (2004).

151

### 152 **3.3 Analyses on core GeoB 9064**

#### 153 **3.3.1 AMS radiocarbon dating**

154 Accelerator mass spectrometry (AMS) dating was performed at the Leibniz Laboratory for  
155 Age Determinations and Isotope Research (University of Kiel, Germany; Nadeau et al.,  
156 1997) and at the Poznań Radiocarbon Laboratory (Poznań, Poland). AMS  $^{14}\text{C}$  dates were  
157 determined on ~8 mg calcium carbonate of mixed planktonic foraminifera. All ages were  
158 corrected for  $^{13}\text{C}$  and a mean ocean reservoir age of 400 years (Bard, 1988). AMS  $^{14}\text{C}$  ages



159 were converted to calendar years using the CALPAL 2007 Hulu software (Joeris and  
160 Weninger, 1998) and are reported as calendar years before present (ka; Table 3).

161

### 162 **3.3.2 Stable oxygen isotopes**

163 The stable oxygen isotope ( $\delta^{18}\text{O}$ ) composition of the planktonic foraminifera  
164 *Neogloboquadrina pachyderma* (dex.) was measured with a Finnigan MAT 251 mass  
165 spectrometer (Isotope Laboratory of the Department of Geosciences, University of Bremen,  
166 Germany). The isotopic composition was measured on the  $\text{CO}_2$  gas evolved by treatment with  
167 phosphoric acid at a constant temperature of 75°C. A working standard (Burgbrohl  $\text{CO}_2$  gas)  
168 was applied, which has been calibrated against PDB by using the NBS18, 19 and 20 standards.  
169 Consequently, all  $\delta^{18}\text{O}$  data presented here are given relative to the PDB standard. Analytical  
170 standard deviation was about  $\pm 0.07\text{‰}$ .

171

### 172 **3.3.3 Grain-size analysis and end-member modelling**

173 Grain sizes were measured on bulk and terrigenous material using a Malvern Instruments  
174 Mastersizer 2000 (Hydraulic Research Laboratory, Borgerhout, Belgium), which determines  
175 particle grain sizes between 0.26  $\mu\text{m}$  and 2 046  $\mu\text{m}$  grouped into 66 size classes. The  
176 terrigenous sediment fraction was obtained by treating bulk sediment with  $\text{H}_2\text{O}_2$  (30% at  
177 85°C) and HCl (10% at 100°C) to remove organic carbon and calcium carbonate, respectively.  
178 The sediments contained negligible amounts of biogenic opal, and microscopic analyses  
179 revealed that the applied method successfully removed all biogenic constituents. Finally, the  
180 samples were suspended in demineralised water by stirring and ultrasonic dispersion before  
181 analysis.

182

183 The terrigenous fraction of deep-sea sediments in the ocean is considered a mixture of ice-  
184 rafted, aeolian, and fluvial transported sediments. End-member modelling allows the

185 distinction between possible lithic subpopulations of the grain-size spectrum (Weltje, 1997)  
186 that can be assigned to different sediment transport mechanisms (e.g., Stuut et al., 2002;  
187 Holz et al., 2007). To estimate the minimum number of end-members (EM) required for a  
188 satisfactory approximation of the data, the coefficients of determination were calculated.  
189 These coefficients represent the proportion of the variance of each grain-size class that can  
190 be reproduced by the approximated data. This proportion is equal to the squared  
191 correlation coefficient ( $r^2$ ) of input variables and their approximated values (Weltje, 1997;  
192 Prins and Weltje, 1999). As the terrigenous sediment fraction from the southern GoC is  
193 relatively fine-grained (<170  $\mu\text{m}$ ), the number of input variables for the end-member model  
194 of core GeoB 9064 was reduced from 66 to 47 classes in the range of 0.29-170  $\mu\text{m}$ .

195

#### 196 **3.3.4. Planktonic foraminiferal assemblage**

197 The analysis for planktonic foraminiferal relative abundance counts is based on the  
198 >150  $\mu\text{m}$  fraction. For each sample a minimum of ~200 specimens were identified following  
199 the taxonomy of planktonic foraminifera proposed by Hemleben et al. (1989). For  
200 *Neogloboquadrina pachyderma* the relative abundances of right (dex.) and left (sin.) coiling  
201 individuals were determined, and the two forms were treated as individual species. The  
202 data are represented as percentages of total planktonic foraminiferal number.

203

### 204 **4. Results**

#### 205 **4.1. U-series dating**

206 All selected coral fragments indicated minor to moderate physico-chemical alteration or  
207 dissolution which may disturb U-series ages. Initial  $\delta^{234}\text{U}_0$  values are variable and range  
208 between  $125.9 \pm 2.7\text{‰}$  to  $187.1 \pm 2.6\text{‰}$  (Table 2, Fig. 2). Measured  $^{232}\text{Th}$  concentrations are  
209 small (<10  $\text{ng g}^{-1}$ ) for 75% of all samples (Fig. 2) but clearly specimens of *Madrepora oculata*  
210 reveal more residual Th than *Lophelia pertusa* (Table 2). This is a consequence of the

211 cleaning procedure as the thinner polyps and more fragile skeleton of *M. oculata* is by far  
212 more difficult to clean. However, Th contamination is negligible since in general the  
213  $^{230}\text{Th}/^{232}\text{Th}$  activity ratios are  $>1\ 000$ .

214

215 Calculated U-series ages from all investigated coral sites in the GoC range from 9.2 ka to  
216 more than 400 ka (Fig. 3). Two samples from core GeoB 12101 could not be dated due to  
217 above equilibrium radioactive isotopic composition indicating U-series open system  
218 behaviour. More than 90% of all obtained ages correspond to glacial periods (Marine  
219 Isotope Stage (MIS) 2 back to MIS12), and 70% of these glacial coral ages cluster within the  
220 last glacial (MIS2-4) (Fig. 3). With regard to the initial  $\delta^{234}\text{U}_0$ , it is evident that the scatter  
221 increases largely beyond a coral age of 150 ka which is clearly indicative of increasing U-  
222 series system opening (Thompson et al., 2003; Scholz et al., 2004; Frank et al., 2006;  
223 Robinson et al., 2006). Consequently, those ages are less precise than the measured  
224 uncertainty would suggest which has to be taken in consideration for our data  
225 interpretation. Corals ages between 14 and 60 ka yield a mean initial  $\delta^{234}\text{U}_0$  of  $143.2\pm 2.3\text{‰}$   
226 ( $n=22$ ,  $2\sigma$  standard deviation), which is slightly lower than measured in modern corals and  
227 seawater (146.6-149.6‰; Delanghe et al., 2002; Robinson et al., 2004). Thus either corals  
228 suffer from minor U-series system opening, and thus, preferential loss of  $^{234}\text{U}$ , or the glacial  
229 mean value of seawater was slightly lower than compared to today as suggested by Esat et  
230 al. (1999). Overall we consider that within a range of  $149\pm 10\text{‰}$  calculated ages are  
231 representing the chronological ages of the corals within the uncertainty of measurement  
232 (see also Stirling et al., 1998; Robinson et al., 2004; Esat and Yokoyama, 2006). However,  
233 we are aware that a more detailed analysis of the U-series data and uncertainties  
234 considering potential seawater U-isotopic variations, diagenetic alteration and U-series  
235 system opening is needed to improve in particular the quality of coral ages beyond 150 ka.

236

237 **4.2. Age model core GeoB 9064**

238 The age model of core GeoB 9064 for the last ~40 kyr is based on six AMS <sup>14</sup>C age control  
239 points and linear interpolation between these dates (Table 3, Fig. 4). The age model is  
240 supported by the correlation of the δ<sup>18</sup>O measurements of the record (showing heavy δ<sup>18</sup>O  
241 values of 1.5-2.5‰ for the last glacial and light values of <1.0‰ for the Holocene; Fig. 4)  
242 with the δ<sup>18</sup>O record of the GRIP ice core (GRIP Members, 1993). The estimated average  
243 sedimentation rate is ~16 cm ka<sup>-1</sup> (Table 3). Highest sedimentation rates of 18-24 cm ka<sup>-1</sup> occur  
244 during MIS3 and the last deglaciation. Lowest sedimentation rates of 8-9 cm ka<sup>-1</sup> are obtained for  
245 MIS2 and the Holocene (Fig. 4).

246

247 **4.3. Grain size distribution and source**

248 The median grain size of the terrigenous (bulk) fraction of sediment core GeoB 9064 varies  
249 between 5.71 μm (5.93 μm) and 12.03 μm (17.88 μm). The last glacial period and the Younger  
250 Dryas (YD) cold event are characterised by relatively coarse sediment deposition. In contrast,  
251 during the Holocene a distinct and continuous decrease of grain sizes is clearly visible (6-  
252 9 μm) (Fig. 4). A three-end-member model was created (with r<sup>2</sup>=0.77) to describe the grain  
253 size data set of core GeoB 9064. The grain size distributions of the three end members are all  
254 unimodal, well-sorted and have relatively fine modal grain sizes with 25 μm for EM1, 16 μm  
255 for EM2, and 5 μm for EM3. Several sedimentological studies confirmed that aeolian  
256 sediments deposited in the deep-sea close to the continent are coarser grained than  
257 hemipelagic sediments with terrigenous sediments with mean grain sizes >6 μm being  
258 generally attributed to aeolian transport, and sediments <6 μm to hemipelagic transport  
259 (Ratmeyer et al., 1999; Prins et al., 2000). In addition, the mean modal sizes of present-day  
260 aeolian dust, collected along a transect of the NW African coast (33°N to 12°S) vary between  
261 8 μm and 42 μm (Stuut et al., 2005). Hence, for core GeoB 9064, the two coarsest end  
262 members of the three-end-member model are considered to be of aeolian origin with EM1

263 interpreted as 'coarse' aeolian dust and EM2 as 'fine' aeolian dust. In contrast, EM3 is  
264 interpreted to result predominantly from fluvial input (Koopmann, 1981; Holz et al., 2007).  
265 During the last glacial, the aeolian content varies considerably between 30% and 60% and  
266 shows in particular during MIS3 rapid fluctuations. Close to the end of the last glacial (~17 ka),  
267 the aeolian content decreases before it increases again up to 60% during the YD. With the  
268 end of the YD (~11.5 ka), the proportion of the aeolian content on the total terrigenous  
269 fraction decreases continuously down to 25% (Fig. 4).

270

271 The EM1/EM2-ratio is considered as a measure for the relative wind intensity (Stuut et al.,  
272 2002). For core GeoB 9064, relatively high wind strength is indicated for the last glacial  
273 showing millennial-scale fluctuations. At ~22 ka, the wind conditions changed dramatically.  
274 Within a time period of 1.5 kyr, wind intensity decreased remarkably by 50% and stayed  
275 low during the entire Holocene (Fig. 4). This is deduced from a reduction of the content of  
276 'coarse' aeolian dust (EM1) to almost zero, whereas the 'fine' aeolian dust (EM2) slightly  
277 increased towards the present.

278

#### 279 **4.4. Planktonic foraminiferal assemblage and abundance**

280 The most abundant species in core GeoB 9064 is *Neogloboquadrina pachyderma* dex.  
281 (27.1%), followed by *Globigerinita glutinata* (21.1%), *Globigerina bulloides* (15.8%), and  
282 *Globorotalia inflata* (12.2%). Together with *Globigerinoides ruber* (5.2%), *Globorotalia*  
283 *scitula* (4.5%), and *N. pachyderma* sin. (4.5%), these species account on average for >90%  
284 of the total planktonic foraminifera.

285

286 Maximum relative abundances of *N. pachyderma* dex. is recorded during the last glacial,  
287 contributing up to 60% of the total planktonic foraminifera fauna. At the end of the last glacial  
288 (15.5-14.5 ka), its relative abundances decreased remarkably down to 10%, followed by an  
289 increase up to 40% during the YD. At the end of the YD (~11.5 ka), relative abundances of *N.*

290 *pachyderma* dex. significantly decreased down to <5% (Fig. 5). A similar trend is indicated for  
291 *N. pachyderma* sin., although it shows comparably lower abundances below 18%. Another  
292 abundant species during the last glacial was *G. glutinata* with relative abundances of 10-40%.  
293 During the course of the Holocene, its contribution was rather low with minimum rates of  
294 <10% except for the period between 10 and 8.5 ka, with relative abundances of up to 28%. An  
295 opposite trend to the above mentioned species is observed for *G. bulloides*. Relatively low  
296 abundance occurred during the last glacial (<20%), whereas during the Holocene, its relative  
297 contribution to the total fauna increased to >20%. In particular between 8.5 and 2 ka, *G.*  
298 *bulloides* was the most common species within the planktonic foraminiferal fauna with  
299 relative abundance of 30-48%. Between 40 and 18 ka, abundances of *G. inflata* were below  
300 20%, and increased up to 38% until the onset of the YD. During the Holocene, its abundances  
301 varied between 8% and 20%. One distinct minimum (<10%) of *G. inflata* abundance is  
302 indicated between 10 and 8.5 ka that mirrors the concomitant maxima of *G. glutinata*.  
303 Contributions of *G. scitula* to the total fauna was rather moderate for most of the last glacial,  
304 and decreased remarkably around 18 ka to <5%, and remained low thereafter (Fig. 5). During  
305 the last glacial and until the end of the YD (~11.5 ka), *G. ruber* shows a low abundance of 0-  
306 10% that increased to 10-25% during the Holocene. *Globigerinoides sacculifer* was even  
307 absent during the last glacial. This species is exclusively found during the Holocene with  
308 relative abundances of up to 7.5% (Fig. 5).

309

## 310 **5. Discussion**

### 311 **5.1. Glacial coral growth phases in the Gulf of Cádiz**

312 During the past years, much effort has been invested into dating cold-water corals from  
313 various sites along the NE Atlantic margin. The most comprehensive data set of coral ages  
314 exists for the Irish margin and reveals that coral growth in this area is restricted to the  
315 Holocene and prior interglacial periods (Frank et al., 2005; Rüggeberg et al., 2007; de Haas

316 et al., 2009; Frank et al., 2009). In contrast, for coral sites south of 50°N the data set of coral  
317 ages is rather scattered. However, the available dates suggest that the major phase of coral  
318 growth along the French, Iberian and Moroccan margins coincide with the last glacial  
319 period (Taviani et al., 1991; Schröder-Ritzrau et al., 2005; Wienberg et al., 2009).

320

321 For the GoC, it was shown that the reef-forming coral species *Lophelia pertusa* and  
322 *Madrepora oculata* have been restricted to a period between 12 and 45 ka (Wienberg et al.,  
323 2009). This preliminary result is confirmed by our data. In addition, the U/Th dates  
324 presented here show that major phases of coral growth in the GoC are not solely restricted  
325 to the last glacial but also to prior glacial periods (back to MIS12), whereas during  
326 interglacials coral growth seems to be reduced or even absent (Fig. 2).

327

328 Most conspicuous is that the widespread decline of the coral ecosystems in the GoC during  
329 the YD cold reversal (12.9–11.5 ka) corresponds to the re-start of coral mound formation on  
330 Rockall Bank and the re-establishment of coral mound growth along the slopes of the  
331 Porcupine Seabight at around 11 ka (Frank et al., 2009). Regarding this pattern, we suggest  
332 that at the transition of the last glacial-interglacial, a latitudinal shift of areas with optimum  
333 cold-water coral growth conditions towards the northern NE Atlantic occurred that was  
334 most probably related to dramatic changes of the oceanographic and environmental  
335 conditions caused by climate change. Moreover, this northward shift happened rapidly over  
336 just a few hundreds of years and over a distance of 2 000-2 500 km (GoC to Irish margin).

337

338 Unfortunately, we still lack detailed understanding of the reproductive ecology and larval  
339 dispersal mode of scleractinian cold-water corals. Histological studies show that the  
340 cosmopolitan species *L. pertusa* exhibits an annual gametogenic cycle with spawning  
341 around January/February (Waller and Tyler, 2005). The widespread occurrence of *L. pertusa*  
342 and the rapid colonisation of man-made structures such as oil rigs (25 mm year<sup>-1</sup>; Bell and

343 Smith, 1999), point to a dispersive planula larva being capable to remain in the water  
344 column for several weeks.

345

## 346 **5.2. Driving factors for coral growth**

347 A combination of environmental and oceanographic conditions is required to promote a  
348 sustained development of cold-water coral ecosystems. Cold-water corals require (1) hard  
349 substrate to settle on, (2) protection against burial to grow, and (3) sufficient food supply.  
350 Therefore, they predominate in areas where strong currents prevail that reduce deposition  
351 of fine-grained sediments and supply large quantities of food (Roberts et al., 2006). Today,  
352 thriving coral ecosystems occur in high concentrations in areas that are characterised by  
353 enhanced primary production in the surface waters of eutrophic systems, allowing a  
354 considerable part of the new production to be transported to the seafloor. In addition, tidal  
355 currents and internal waves have been identified (1) to enhance concentrations of organic  
356 matter at the shelf edge and (2) to transport fresh food particles to and through the cold-  
357 water coral reefs (Frederiksen et al., 1992; White et al., 2005; White et al., 2007). Recently,  
358 Dullo et al. (2008) indicated for the Celtic and Nordic margins that living cold-water corals  
359 occur within the density envelope of sigma-theta ( $\sigma_\theta$ )=27.35-27.65 kg m<sup>-3</sup> emphasising the  
360 importance of physical boundary conditions. Finally, the world's most common cold-water  
361 coral species *Lophelia pertusa* tends to be associated with oceanic water masses with a  
362 temperature of 4-12°C (Roberts et al., 2006), and even up to 14°C in the Mediterranean Sea  
363 (Taviani et al., 2005; Freiwald et al., 2009), salinities between 31.7 and 38.78 (Freiwald et  
364 al., 2004; Davies et al., 2008), and oxygen concentrations of 4.3-7.2 ml l<sup>-1</sup> (for the NE  
365 Atlantic; Davies et al., 2008).

366

367 For the GoC, all these requirements must have been fulfilled during glacial periods as cold-  
368 water corals were widespread during these times. During interglacial periods, these optimal  
369 environmental and oceanographic conditions must have been changed dramatically



370 resulting in a widespread (gulf-wide) demise of the formerly thriving corals. As our obtained  
371 coral ages mainly cluster within the last glacial (~70%), the environmental and  
372 oceanographic changes of the GoC, focussing on the last glacial-interglacial cycle, are  
373 discussed in detail to identify the main forcing factors for coral growth in the GoC.

374

### 375 **5.2.1 Effects of increased palaeo-productivity on cold-water coral growth**

376 Strong vertical fluxes of labile organic matter, as often found in eutrophic regions, result in  
377 rich benthic fauna (e.g., De Stigter et al., 1998; Schmiedl et al., 2000; Fontanier et al., 2002).  
378 In the NE Atlantic, seasonal algae blooms that sink rapidly to the deep-sea floor can even  
379 have a positive effect on the reproductive biology of benthic invertebrates (Billett et al.,  
380 1983; Thiel et al., 1989; Tyler et al., 1992), a relationship which is also hypothesised for  
381 *Lophelia pertusa* and *Madrepora oculata* thriving along the Irish margin (Waller and Tyler,  
382 2005). Thus, enhanced productivity is a pre-requisite for a sustained development of  
383 healthy cold-water coral ecosystems. Indeed, regions with enhanced primary production as  
384 deduced from satellite-based observations of the chlorophyll content in surface waters  
385 (Behrenfeld et al., 2005) seem to mirror the recent distribution of thriving coral sites in the  
386 NE Atlantic.

387

388 Certain species of planktonic foraminifera strongly depend on primary productivity in the  
389 modern ocean (Hemleben et al., 1989), and hence downcore variations of the abundance of  
390 planktonic foraminiferal species within sedimentary records can be applied to assess  
391 palaeo-productivity conditions (e.g., Ivanova et al., 2003). In this context, the  
392 environmental constraints of the most abundant foraminiferal species identified for the  
393 GoC are reviewed in detail.

394

395 *Globigerina bulloides* mainly thrives in the surface mixed layer above the thermocline and  
396 prefers relatively cold and nutrient-rich waters (e.g., Ganssen and Kroon, 2000; Chapman,

397 2010). Moreover, this species preferably occurs in areas along the Iberian and NW African  
398 margins that are characterised by pronounced seasonal upwelling, and thus, by high  
399 phytoplankton density and prey abundance (Salgueiro et al., 2008; Wilke et al., 2009). The  
400 opportunistic and cosmopolitan species *Globigerinita glutinata* is also strongly associated  
401 with the increase in productivity during spring bloom events in the North Atlantic  
402 (Chapman, 2010). However, the distribution of this species is found to be even more  
403 significantly associated with productivity than that of *G. bulloides*, which can be explained  
404 by its diet that preferentially consists of diatoms (Bé and Tolderlund, 1971; Hemleben et al.,  
405 1989; Schiebel et al., 2001). The sub-polar species *Neogloboquadrina pachyderma* dex.  
406 prefers colder waters than *G. bulloides* (Bé and Tolderlund, 1971). Off the northern Iberian  
407 margin, high percentages of this species have been related to increased productivity  
408 generated by high river runoff (Salgueiro et al., 2008). In the GoC, *G. glutinata* and  
409 *N. pachyderma* dex. clearly dominate the foraminiferal assemblage during the last glacial  
410 with relative abundances of 55 to 75% (Fig. 5), thus pointing to rather nutrient-rich and cold  
411 conditions compared to the following Holocene when both species account for only ~10%.  
412 However, although *G. bulloides* is regarded as an indicator for nutrient enriched conditions  
413 it shows an opposite trend compared to the other two species.

414

415 *Globorotalia inflata* is considered a non-upwelling species and high relative abundances of  
416 this species in the North Atlantic coincide with oligotrophic waters (Pflaumann et al., 2003;  
417 Salgueiro et al., 2008). The two surface-dwelling species *Globigerinoides ruber* and  
418 *Globigerinoides sacculifer* show a preference towards oligotrophic conditions as well (e.g.,  
419 Ivanova et al., 2003; Mohtadi et al., 2007). These species prefer warm and well stratified  
420 surface waters (Duplessy et al., 1981; Stoll et al., 2007; Chapman, 2010). For the NE  
421 Atlantic, a significant increase in the relative abundances of *G. sacculifer* is observed when  
422 surface stratification is at a maximum and high sea surface temperatures prevail (Chapman,  
423 2010). The significant increase of *G. ruber* and *G. sacculifer* after the YD cold event as found in

424 our record (Fig. 5) thus indicates such warm and well stratified conditions in the GoC during  
425 the Holocene.

426

427 Taking all these findings for the NE Atlantic into account, *G. sacculifer*, *G. ruber* and *G.*  
428 *inflata* are inferred to represent a low-productivity assemblage, whereas *G. glutinata*,  
429 *G. bulloides* and *N. pachyderma* dex. are grouped as indicators for enhanced productivity.  
430 Similar to the approach of Stoll et al. (2007), we calculated the ratio of both assemblages  
431 and interpreted this ratio as an indicator of productivity (Fig. 4f), regardless of their affinity  
432 to upwelling processes. This ratio clearly shows that during the last glacial palaeo-  
433 productivity was overall enhanced in the GoC, which is in particular expressed by high  
434 relative abundances of *G. glutinata* (Fig. 5). Following the end of the last glacial, this ratio  
435 significantly changed towards more oligotrophic conditions (Fig. 4).

436

### 437 **5.2.2 Implications of frontal upwelling on glacial productivity in the GoC**

438 This pattern of eutrophic conditions during the last glacial and oligotrophic conditions  
439 during the Holocene found for the GoC might be explained by a shift of the Azores Front  
440 (Rogerson et al., 2004). The Azores Front marks a zone of strong hydrographic transition  
441 associated with enhanced biological production caused by locally intense upwelling (Alves  
442 and DeVerdière, 1999). Today, the easternmost extension of the Azores Front is situated at  
443 30°N off the Moroccan margin (Gould, 1985; Schiebel et al., 2002), and hence, does not  
444 penetrate into the GoC that extends from 37°N to 33°N (Fig. 1). But there is evidence that  
445 the Azores Front shifted northward and thus penetrated eastward into the GoC prior to 16  
446 ka and during the YD (Rogerson et al., 2004). Rogerson et al. (2004) indicated this glacial  
447 shift of the Azores Front towards the GoC by high abundances of the planktonic foraminifer  
448 *Globorotalia scitula* in their records. This deep-dwelling species (100-700 m water depth)  
449 (Schiebel et al., 2002) is used as an indicator for cool surface waters and enhanced vertical  
450 mixing at temperate latitudes (e.g., Thunell and Reynolds, 1984; Perez-Folgado et al., 2003).

451 Today *G. scitula* is found in high numbers in the Azores Front where upwelling causes high  
452 productivity (Schiebel et al., 2002), but it is almost absent in the GoC (Rogerson et al.,  
453 2004). The record of core GeoB 9064 shows that *G. scitula* is common prior to the Last  
454 Glacial Maximum (LGM), but is rare throughout the Holocene (Fig. 5) pointing to enhanced  
455 productivity during the last glacial caused by frontal upwelling.

456

### 457 **5.2.3 Fertilisation effect of aeolian dust**

458 Besides the effect of locally intensified upwelling that likely occurred in the GoC during the  
459 last glacial also the high input of aeolian dust might have significantly enhanced glacial  
460 productivity in the area. Grain size data from various sediment cores in the GoC, including  
461 our data (Fig. 4), show that during the last glacial mean grain sizes were rather coarse  
462 compared to the following Holocene (e.g., Rogerson et al., 2005; Voelker et al., 2006). Up to  
463 now, these grain size variations have been primarily attributed to changes in the strength of  
464 the prevailing bottom currents implying that bottom current strength was enhanced during  
465 the last glacial probably caused by a shift and intensification of the MOW's flow pathway  
466 (Schönfeld and Zahn, 2000; Rogerson et al., 2005; Voelker et al., 2006). Another common  
467 finding for the GoC is a rather low Holocene sedimentation rate (e.g., Rogerson et al., 2005;  
468 Voelker et al., 2006). Rogerson et al. (2005) estimated a Holocene accumulation rate that is  
469 only one fifth of that of the last glacial, and thus is in agreement with our estimated rates  
470 (Fig. 4). They assumed that this tremendous change in sedimentation rate was caused by a  
471 higher sediment supply prior to the last deglaciation but without indicating the major  
472 source of sediments supplied to the GoC.

473

474 However, this study shows that the variations in grain size and sedimentation rate as found  
475 for the GoC are rather the result of changes in the source of the terrigenous sediments and  
476 the amount of sediment input. Our grain size data clearly reveal that during the last glacial  
477 the deposition of aeolian transported sediments prevailed in the GoC (Fig. 4). During this

478 time rather arid and cold conditions prevailed over the NW African continent (Gasse, 2000),  
479 and the intensity of the northern trade winds, which transport the aeolian dust, was  
480 enhanced especially from about 36°N to 24°N (Sarnthein et al., 1981; Hooghiemstra et al.,  
481 1987; Moreno et al., 2002). This is supported by our record showing that wind strength off  
482 Morocco (35°N) was significantly enhanced during the last glacial (Fig. 4). With the end of  
483 the YD, the proportion of the aeolian content on the total terrigenous fraction decreased  
484 continuously from 60 to 25% (Fig. 4), corresponding to the African humid period, which is  
485 known to be characterised by a relatively humid and green Sahara with significantly lower  
486 amounts of aeolian dust being produced (e.g., deMenocal et al., 2000; Gasse, 2000). The  
487 African humid period terminated at 5.5 ka and the area of the Saharan desert returned to a  
488 state of hyperarid conditions (deMenocal et al., 2000). However, wind strength remained  
489 relatively low compared to the strong glacial trade winds (Hooghiemstra et al., 1987) and  
490 dust fluxes have been estimated to be today 2-4 times lower compared to the LGM  
491 (Grousset et al., 1998). Also our data show no significant increase of the input of aeolian  
492 dust in the GoC after 5.5 ka until today (Fig. 4).

493

494 The large input of aeolian dust during the last glacial coincides with a prosperous cold-  
495 water coral community in the GoC (Fig. 4). The link between dust input and coral prosperity  
496 was probably established by a simple fertilisation effect. During periods of enhanced  
497 Saharan dust input over the NE Atlantic, the supply of iron and manganese to the surface  
498 ocean is enhanced as well (de Jong et al., 2007) which promotes primary production in the  
499 surface waters (e.g., Boyd et al., 2000), and as a consequence, also might increase food  
500 availability for the bathyal cold-water corals.

501

#### 502 **5.2.4 Limitation of water temperatures on the prosperity of cold-water corals**

503 The planktonic foraminiferal abundance data of core GeoB 9064 is consistent with the  
504 thermal history of the LGM and deglaciation. The general warming of the North Atlantic at

505 the transition from the last glacial to the Holocene is reflected by a considerable increase in  
506 the abundance of *G. ruber* and *G. sacculifer* and a concurrent decrease in abundance of *N.*  
507 *pachyderma* dex., which is even more pronounced after the YD cold reversal (Fig. 5). This  
508 pattern is in agreement with other foraminiferal fauna records from the GoC (Sierro et al.,  
509 1999; Rogerson et al., 2004). The change from rather cool towards warm surface waters  
510 after the end of the YD was most likely accompanied by a change in subsurface  
511 temperatures in intermediate water depths, thus having an impact on the bathyal cold-  
512 water corals. Regarding the average temperatures of the intermediate water masses  
513 prevailing in the GoC (NACW: ~12°C, Ait-Ameur and Goyet, 2006; MOW: 10.5-12°C, Fusco et  
514 al., 2008), it becomes obvious that at least today water temperatures are at the very upper  
515 tolerance for reef-forming scleractinian cold-water corals such as *Lophelia pertusa* (12°C;  
516 Roberts et al., 2006). Moreover, dendrophylliid coral species that prefer rather warm  
517 conditions compared to *L. pertusa* seem to have been more common during the late  
518 Holocene (Wienberg et al., 2009).

519

## 520 **6. Conclusion**

521 This study clearly shows that the occurrence of cold-water corals in the GoC is dominant  
522 within the last glacial and prior glacial periods and that hardly any cold-water corals exist in  
523 this region during interglacials. Moreover, it could be identified that at the end of the YD  
524 cold event a shift from eutrophic to oligotrophic and warm conditions have been  
525 responsible for the demise of the formerly thriving coral ecosystems. The enhanced  
526 productivity conditions during the last glacial have been most probably caused by (1) an  
527 enhanced input of aeolian dust and (2) a shift of the Azores Fronts towards the GoC causing  
528 locally intense upwelling. Both factor supported enhanced primary productivity in the GoC,  
529 and thus resulted in enhanced food availability for the corals. By comparing our data set for  
530 the GoC with coral ages from the Norwegian and Irish margins that reveal a sustained  
531 prosperity of coral ecosystems right after the YD, it appears that a northward shift of areas

532 with optimum cold-water coral growth conditions took place during the transition from the  
533 last glacial to the recent interglacial. The cold-water corals responded very rapidly to  
534 climate change over just a few hundreds of years, and it is most likely that in the course of  
535 global warming going along with dramatic changes in the environmental setting this  
536 northward trend will further continue.

537

## 538 **Acknowledgements**

539 *The research leading to these results (U/Th and radiocarbon dates) has received funding from the European*  
540 *Community's Seventh Framework Programme (FP7/2007-2013) under the HERMIONE project, grant agreement*  
541 *n° 226354. In addition, this work is part of CARBONATE (palaeo-environmental reconstructions), an ESF*  
542 *EUROCORES integrated project as part of the EuroMARC project cluster funded by the DFG. K.M. Mertens is a*  
543 *Postdoctoral Researcher funded by the FWO. M. Marchant acknowledges the Dirección de Investigación and*  
544 *Departamento de Zoología at the University of Concepción (Chile) and the German Academic Exchange Service*  
545 *(DAAD). On-board assistance by ship and scientific team during cruises SO175 with RV Sonne (2003), 64PE229*  
546 *with RV Pelagia (2004) and MSM01-3 with RV Maria S. Merian (2006) is acknowledged. O. Pfannkuche, J.*  
547 *Schönfeld and L. Maignien are kindly thanked for their great scientific support during cruise MSM01-3. We*  
548 *further acknowledge the support of the staff of the LSCE Gif-sur-Yvette (E. Douville, E. Sallé, C. Noury), the*  
549 *German Leibniz Laboratory for Age Determination and Isotope Research (University of Kiel, Germany), and the*  
550 *Poznan Radiocarbon Laboratory (Poznan, Poland) in U/Th and radiocarbon dating as well as the staff of the*  
551 *UGhent (M. Verreth, A. Raes, F. Mostaert) in sample preparation and grain size analysis. Finally, A. Eisenhauer,*  
552 *M. Mohtadi and two anonymous reviewers are kindly thanked for helpful discussions and comments.*

553

## 554 **References**

- 555 Ait-Ameur, N., Goyet, C., 2006. Distribution and transport of natural and anthropogenic CO<sub>2</sub> in the Gulf of Cádiz.  
556 *Deep-Sea Res. II* 53, 1329–1343.
- 557 Alves, M., DeVerdière, A.C., 1999. Instability dynamics of a subtropical jet and applications to the Azores Front  
558 current system: Eddydriven mean flow. *J. Physic. Oceanogr.* 29, 837-864.
- 559 Ambar, I., Armi, L., Bower, A., Ferreira, T., 1999. Some aspects of time variability of the Mediterranean outflow.  
560 *Deep-Sea Res.* 26A, 1109-1136.
- 561 Bard, E., 1988. Correction of accelerator mass spectrometry <sup>14</sup>C ages measured in planktonic foraminifera:  
562 *Paleoceanographic implications. Paleoceanography* 3, 635-645.
- 563 Baringer, M.O., Price, J.F., 1999. A review of the physical oceanography of the Mediterranean outflow. *Mar.*  
564 *Geol.* 155, 63-82.
- 565 Bé, A.W.H., Tolderlund, D.S., 1971. Distribution and ecology of living planktonic foraminifera in surface waters of  
566 the Atlantic and Indian Oceans. In: Funel, B.M., Riedel, W.R. (Eds.), *The Micropaleontology of Oceans.*  
567 Cambridge University Press, pp. 105-149.
- 568 Behrenfeld, M.J., Boss, E., Siegel, D.A., Shea, D.M., 2005. Carbon-based ocean productivity and phytoplankton  
569 physiology from space. *Glob. Biogeochem. Cycl.* 19, GB1006, doi:10.1029/2004GB002299.
- 570 Bell, N., Smith, J.E., 1999. Coral growing on North Sea oil rigs. *Nature* 402, 601.
- 571 Billett, D.S.M., Lampitt, R.S., Rice, A.L., Mantoura, R.F.C., 1983. Seasonal sedimentation of phytoplankton to the  
572 deep-sea benthos. *Nature Geosci.* 302, 520-522.
- 573 Boyd, P.W., Watson, A.J., Law, C.S., Abraham, E.R., Trull, T., Murdoch, R., Bakker, D.C.E., Bowie, A.R., Buesseler,  
574 K.O., Chang, H., Charette, M., Croot, P., Downing, K., Frew, R., Gall, M., Hadfield, M., Hall, J., Harvey, M.,  
575 Jameson, G., LaRoche, J., Liddicoat, M., Ling, R., Maldonado, M.T., McKay, R., Nodder, S., Pickmere, S.,  
576 Pridmore, R., Rintoul, S., Safi, K., Sutton, P., Strzepek, R., Tanneberger, K., Turner, S., Waite, A., Zeldis, J., 2000.

577 *A mesoscale phytoplankton bloom in the polar Southern Ocean waters stimulated by iron fertilization. Nature*  
578 *407, 695-702.*

579 Carton, X., Chérubin, L., Paillet, J., Morel, Y., Serpette, A., Le Cann, B., 2002. Meddy coupling with a deep cyclone  
580 in the Gulf of Cádiz. *J. Mar. Syst.* 32, 13-42.

581 Chapman, M.R., 2010. Seasonal production pattern of planktonic foraminifera in the NE Atlantic Ocean:  
582 Implications for paleotemperature and hydrographic reconstructions. *Paleoceanography* 25, PA1101,  
583 doi:10.1029/2008PA001708.

584 Colman, J.G., Gordon, D.M., Lane, A.P., Forde, M.J., Fitzpatrick, J., 2005. Carbonate mounds off Mauritania,  
585 Northwest Africa: status of deep-water corals and implications for management of fishing and oil exploration  
586 activities. In: Freiwald, A., Roberts, J.M. (Eds.), *Cold-water Corals and Ecosystems*. Springer, Heidelberg, pp.  
587 417-441.

588 Davies, A.J., Wisshak, M., Orr, J.C., Roberts, J.M., 2008. Predicting suitable habitat for the cold-water coral  
589 *Lophelia pertusa* (Scleractinia). *Deep-Sea Res. I* 55, 1048-1062.

590 de Haas, H., Mienis, F., Frank, N., Richter, T.O., Steinbacher, R., de Stigter, H., van der Land, C., van Weering,  
591 T.C.E., 2009. Morphology and sedimentology of (clustered) cold-water coral mounds at the south Rockall  
592 Trough margins, NE Atlantic Ocean. *Facies* 55, 1-26.

593 de Jong, J.T.M., Boyé, M., Gelado-Caballero, M.D., Timmermans, K.R., Veldhuis, M.J.W., Nolting, R.F., van den  
594 Berg, C.M.G., de Baar, H.J.W., 2007. Inputs of iron, manganese and aluminium to surface waters of the  
595 Northeast Atlantic Ocean and the European continental shelf. *Mar. Chem.* 107, 120-142.

596 De Stigter, H.C., Jorissen, F.J., Vand der Zwaan, G.J., 1998. Bathymetric distribution and microhabitat partitioning  
597 of live (Rose Bengal stained) benthic foraminifera along a shelf to deep sea transect in the southern Adriatic  
598 Sea. *J. Foram. Res.* 28, 40-65.

599 Delanghe, D., Bard, E., Hamelin, B., 2002. New TIMS constraints on the uranium-238 and uranium-234 in  
600 seawaters from the main ocean basins and the Mediterranean Sea. *Mar. Chem.* 80, 79-93.

601 deMenocal, P., Ortiz, J., Guilderson, T., Adkins, J., Sarnthein, M., Baker, L., Yarusinsky, M., 2000. Abrupt onset  
602 and termination of the African Humid Period:: rapid climate responses to gradual insolation forcing. *Quat. Sci.*  
603 *Rev.* 19, 347-361.

604 Dorschel, B., Hebbeln, D., Rüggeberg, A., Dullo, W.-C., 2005. Growth and erosion of a cold-water coral covered  
605 carbonate mound in the Northeast Atlantic during the Late Pleistocene and Holocene. *Earth Planet. Sci. Lett.*  
606 233, 33-44.

607 Douville, E., Sallé, E., Frank, N., Eisele, M., Pons-Branchu, E., Ayrault, S., 2010. Rapid and accurate Th-U dating of  
608 ancient carbonates using Inductively Coupled Plasma-Quadrupole Mass Spectrometry. *Chem. Geol.* 272, 1-11.

609 Duineveld, G.C.A., Lavleye, M.S.S., Berghuis, E.M., 2004. Particle flux and food supply to a seamount cold-water  
610 coral community (Galicia Bank, NW Spain). *Mar. Ecol. Prog. Ser.* 277, 13-23.

611 Dullo, C., Flögel, S., Rüggeberg, A., 2008. Cold-water coral growth in relation to the hydrography of the Celtic and  
612 Nordic European continental margin. *Mar. Ecol. Prog. Ser.* 371, 165-176.

613 Duplessy, J.C., Bé, A.W., Blanc, P.L., 1981. Oxygen and carbon isotopic composition and biogeographic  
614 distribution of planktonic foraminifera in the Indian Ocean. *Palaeogeogr. Palaeoclimat. Palaeoecol.* 33, 9-46.

615 Eisele, M., Hebbeln, D., Wienberg, C., 2008. Growth history of a cold-water coral covered carbonate mound -  
616 Galway Mound, Porcupine Seabight, NE-Atlantic. *Mar. Geol.* 253, 160-169.

617 Esat, T.M., McCulloch, M.T., Chappell, J., Pillans, B., Omura, A., 1999. Rapid fluctuations in sea level recorded at  
618 Huon Peninsula during the penultimate deglaciation. *Science* 283, 197-201.

619 Esat, T.M., Yokoyama, Y., 2006. Variability in the uranium isotopic composition of the oceans over glacial-  
620 interglacial timescales. *Geochim. Cosmochim. Acta* 70, 4140-4150.

621 Fietzke, J., Liebetrau, V., Eisenhauer, A., Dullo, W.-C., 2005. Determination of uranium isotope ratios by multi-  
622 static MIC-ICP-MS: method and implementation for precise U- and Th-series isotopes. *J. Anal. Atomic Spectrom.*  
623 20, 395-401.

624 Fontanier, C., Jorissen, F.J., Licari, L., Alexandre, A., Anshutz, P., Carbonel, P., 2002. Live benthic foraminiferal  
625 faunas from the Bay of Biscay: faunal density, composition, and microhabitats. *Deep-Sea Res. I* 49, 751-785.

626 Fosså, J.H., Lindberg, B., Christensen, O., Lundälv, T., Svellingen, I., Mortensen, P.B., Alsvag, J., 2005. Mapping of  
627 *Lophelia* reefs in Norway: experiences and survey methods. In: Freiwald, A., Roberts, J.M. (Eds.), *Cold-water*  
628 *Corals and Ecosystems*. Springer, Heidelberg, pp. 359-391.

629 Foubert, A., Depreiter, D., Beck, T., Maignien, L., Pannemans, B., Frank, N., Blamart, D., Henriët, J.-P., 2008.  
630 Carbonate mounds in a mud volcano province off north-west Morocco: key to processes and controls. *Mar.*  
631 *Geol.* 248, 74-96.

632 Frank, N., Paterne, M., Ayliffe, L., van Weering, T.C.E., Henriët, J.-P., Blamart, D., 2004. Eastern North Atlantic  
633 deep-sea corals: tracing upper intermediate water  $\Delta^{14}\text{C}$  during the Holocene. *Earth Planet. Sci. Lett.* 219, 297-  
634 309.

635 Frank, N., Lutringer, A., Paterne, M., Blamart, D., Henriët, J.-P., van Rooij, D., van Weering, T.C.E., 2005. Deep-  
636 water corals of the northeastern Atlantic margin: carbonate mound evolution and upper intermediate water  
637 ventilation during the Holocene. In: Freiwald, A., Roberts, J.M. (Eds.), *Cold-water Corals and Ecosystems*.  
638 Springer, Heidelberg, pp. 113-133.



- 639 Frank, N., Turpin, L., Cabioch, G., Blamart, D., Tressens-Fedou, M., Colin, C., Jean-Baptiste, P., 2006. Open system  
640 U-series ages of corals from a subsiding reef in New Caledonia: Implications for sea level changes, and  
641 subsidence rate. *Earth Planet. Sci. Lett.* 249, 274-289.
- 642 Frank, N., Ricard, E., Lutringer-Paque, A., van der Land, C., Colin, C., Blamart, D., Foubert, A., Van Rooij, D.,  
643 Henriët, J.-P., de Haas, H., van Weering, T.C.E., 2009. The Holocene occurrence of cold-water corals in the NE  
644 Atlantic: Implications for coral carbonate mound evolution. *Mar. Geol.* 266, 129-142.
- 645 Frederiksen, R., Jensen, A., Westerberg, H., 1992. The distribution of scleratinian coral *Lophelia pertusa* around  
646 the Faroe Islands and the relation to intertidal mixing. *Sarsia* 77, 157-171.
- 647 Freiwald, A., Fosså, J.H., Grehan, A., Koslow, T., Roberts, J.M., 2004. *Cold-water Coral Reefs*. UNEP-WCMC,  
648 Biodiversity Series 22, Cambridge, UK, p. 84.
- 649 Freiwald, A., Beuck, L., Rüggeberg, A., Taviani, M., Hebbeln, D., R/V Meteor Cruise M70-1 participants, 2009. The  
650 white coral community in the central Mediterranean Sea revealed by ROV surveys. *Oceanography* 22, 58-74.
- 651 Fusco, G., Artale, V., Cotroneo, Y., Sannino, G., 2008. Thermohaline variability of Mediterranean Water in the  
652 Gulf of Cádiz, 1948-1999. *Deep-Sea Res. I* 55, 1624-1638.
- 653 Ganssen, G., Kroon, D., 2000. The isotopic signature of planktonic foraminifera from the NE Atlantic surface  
654 sediments: implications for the reconstruction of past oceanic conditions. *J. Geol. Soc. London* 157, 693-699.
- 655 García-Lafuente, J., Ruiz, J., 2007. The Gulf of Cádiz pelagic ecosystem: A review. *Prog. Oceanogr.* 74, 228-251.
- 656 García, M., Hernández-Molina, F.J., Llave, E., Stow, D.A.V., León, R., Fernández-Puga, M.C., Diaz del Río, V.,  
657 Somoza, L., 2009. Contourite erosive features caused by the Mediterranean Outflow Water in the Gulf of Cádiz:  
658 Quaternary tectonics and oceanographic implications. *Mar. Geol.* 257, 24-40.
- 659 Gasse, F., 2000. Hydrological changes in the African tropics since the Last Glacial Maximum. *Quat. Sci. Rev.* 19,  
660 189-211.
- 661 Gould, W.J., 1985. Physical oceanography of the Azores Front. *Prog. Oceanogr.* 14, 167-190.
- 662 GRIP Members, 1993. Climate instability during the last interglacial period recorded in the the GRIP ice core.  
663 *Nature* 364, 203-207.
- 664 Grousset, F.E., Parra, M., Bory, A., Martinez, P., Bertrand, P., Shimmield, G., Ellam, R.M., 1998. Saharan wind  
665 regimes traced by the Sr-Nd isotopic composition of subtropical Atlantic sediments: Last Glacial Maximum vs.  
666 today. *Quat. Sci. Rev.* 17, 395-409.
- 667 Hebbeln, D., Wienberg, C., cruise participants, 2008. Report and preliminary results of RV Pelagia cruise  
668 64PE284, Cold-water corals in the Gulf of Cádiz and on Coral Patch Seamount, Portimao - Portimao, 18.02.-  
669 09.03.2008. University of Bremen, Reports of the Department of Geosciences (GeoB) No. 265, p. 90.
- 670 Hemleben, C., Spindler, M., Anderson, O.R., 1989. *Modern Planktonic Foraminifera*. Springer, New York, 363 pp.
- 671 Holz, C., Stuetz, J.B., Meggers, H., Rüdiger, H., 2007. Variability in terrigenous sedimentation processes off  
672 northwest Africa and its relation to climatic changes: inferences from grain-size distributions of a Holocene  
673 marine sediment record. *Sediment. Geol.* 202, 499-508.
- 674 Hooghiemstra, H., Bechler, A., Beug, H.-J., 1987. Isopollen maps for 18,000 years BP of the Atlantic offshore of  
675 Northwest Africa: Evidence for paleowind circulation. *Paleoceanography* 2, 561-582.
- 676 Imbrie, J., Hays, J.D., Martinson, D.G., McIntyre, A., Mix, A.C., Morley, J.J., Pisias, N.G., Prell, W.L., Shackleton,  
677 N.J., 1989. The orbital theory of Pleistocene climate: support from a revised chronology of the marine  $\delta^{18}\text{O}$   
678 record. In: Berger, A. (Ed.), *Milankovitch and Climate*. NATO ASI Series, Dordrecht, pp. 269-305.
- 679 Ivanova, E., Schiebel, R., Singh, A.D., Schmiedl, G., Niebler, H.-S., Hemleben, C., 2003. Primary production in the  
680 Arabian Sea during the last 135000 years. *Palaeogeogr. Palaeoclimat. Palaeoecol.* 197, 61-82.
- 681 Joeris, O., Weninger, B., 1998. Extension of the  $^{14}\text{C}$  calibration curve to ca. 40,000 cal BC by synchronizing  
682 Greenland  $^{18}\text{O}/^{16}\text{O}$  ice core records and North Atlantic foraminifera profiles: A comparison with U/Th coral  
683 data. *Radiocarbon* 40, 495-504.
- 684 Koopmann, B., 1981. Sedimentation von Saharastaub im subtropischen Nordatlantik während der letzten 25.000  
685 Jahre. *Meteor Forschungsgeb.* 35, 23-59.
- 686 Lindberg, B., Berndt, C., Mienert, J., 2007. The Fugløy Reef at 70°N; acoustic signature, geologic, geomorphologic  
687 and oceanographic setting. *Int. J. Earth Sci.* 96, 201-213.
- 688 Machín, F., Pelegrí, J.L., Marrero-Díaz, A., Laiz, I., Ratsimandresy, A.W., 2006. Near-surface circulation in the  
689 southern Gulf of Cádiz. *Deep-Sea Res. II* 53, 1161-1181.
- 690 Mauritzen, C., Morel, J., Paillet, J., 2001. On the influence of Mediterranean water on the central waters of the  
691 North Atlantic Ocean. *Deep-Sea Res.* 44, 1543-1574.
- 692 Mittelstaedt, E., 1991. The ocean boundary along the northwest African coast: Circulation and oceanographic  
693 properties at the sea surface. *Prog. Oceanogr.* 26, 307-355.
- 694 Mohtadi, M., Max, L., Hebbeln, D., Baumgart, A., Krück, N., Jennerjahn, T., 2007. Modern environmental  
695 conditions recorded in surface sediment samples off W and SW Indonesia: Planktonic foraminifera and biogenic  
696 compounds analyses. *Mar. Micropaleontol.* 65, 96-112.
- 697 Moreno, A., Cacho, I., Canals, M., Prins, M.A., Sánchez-Goñi, M.-F., Grimalt, J.O., Weltje, G.J., 2002. Saharan dust  
698 transport and high-latitude glacial climatic variability: The Alboran Sea record. *Quat. Res.* 58, 318-328.
- 699 Nadeau, M.J., Schleicher, M., Grootes, P., Erlenkeuser, H., Grotollong, A., Mous, D.J.W., Sarthain, M., Willkomm,  
700 N., 1997. The Leibniz-Labor AMS facility of the Christian-Albrechts University, Kiel, Germany. *Nucl. Instrum.*  
701 *Methods Phys. Res.* 123, 22-30.
- 702 Ochoa, J., Bray, N.A., 1991. Water mass exchange in the Gulf of Cádiz. *Deep-Sea Res.* 38 (S1), 5465-5503.

- 703 Pelegrí, J.L., Marrero-Díaz, A., Ratsimandresy, A., Antoranz, A., Cisneros-Aguirre, J., Gordo, C., Grisolía, D.,  
704 Hernández-Guerra, A., Láz, I., Martínez, A., Parrilla, G., Pérez-Rodríguez, P., Rodríguez-Santana, A., Sangrà, P.,  
705 2005. Hydrographic cruises off northwest Africa: the Canary Current and the Cape Ghir region. *J. Mar. Syst.* 54,  
706 39-63.
- 707 Perez-Folgado, M., Sierro, F.J., Flores, J.A., Cacho, I., Grimalt, J.O., Zahn, R., Shackleton, N.J., 2003. Western  
708 Mediterranean planktonic foraminifera events and millennial climatic variability during the last 70 kyr. *Mar.*  
709 *Micropaleontol.* 48, 49-70.
- 710 Pflaumann, U., Sarnthein, M., Chapman, M., d'Abreu, L., Funnell, B., Huels, M., Kiefer, T., Maslin, M., Schulz, H.,  
711 Swallow, J., van Kreveld, S., Vautravers, M., Vogelsang, E., Weinelt, M., 2003. Glacial North Atlantic: sea-  
712 surface conditions reconstructed by GLAMAP 2000. *Paleoceanography* 18, 1065.
- 713 Prins, M.A., Weltje, G.J., 1999. End-member modeling of siliciclastic grain-size distributions: the Late Quaternary  
714 record of eolian and fluvial sediment supply to the Arabian Sea and its paleoclimatic significance. In: Harbaugh,  
715 J., Watney, L., Rankey, G., Slingerland, R., Goldstein, R., Franseen, E. (Eds.), *Numerical Experiments in*  
716 *Stratigraphy: Recent Advances in Stratigraphic and Sedimentologic Computer Simulations. SEPM*, pp. 91-111.
- 717 Prins, M.A., Postma, G., Cleveringa, J., Cramp, A., Kenyon, N.H., 2000. Controls on terrigenous sediment supply to  
718 the Arabian Sea during the late Quaternary: the Indus Fan. *Mar. Geol.* 169, 327-349.
- 719 Ratmeyer, V., Balzer, W., Bergametti, G., Chiapello, I., Fischer, G., Wyputta, U., 1999. Seasonal impact of mineral  
720 dust on deep-ocean particle flux in the eastern subtropical Atlantic Ocean. *Mar. Geol.* 159, 241-252.
- 721 Reveillaud, J., Freiwald, A., Van Rooij, D., Le Guilloux, E., Altuna, A., Foubert, A., Vanreusel, A., Olu-Le Roy, K.,  
722 Henriot, J.-P., 2008. The distribution of scleractinian corals in the Bay of Biscay, NE Atlantic. *Facies* 54, 317-331.
- 723 Roberts, J.M., Wheeler, A.J., Freiwald, A., 2006. Reefs of the deep: The biology and geology of cold-water coral  
724 ecosystems. *Science* 312, 543-547
- 725 Robinson, L.F., Belshaw, N.S., Henderson, G.M., 2004. U and Th concentrations and isotope ratios in modern  
726 carbonates and waters from the Bahamas. *Geochim. Cosmochim. Acta* 68, 1777-1789.
- 727 Robinson, L.F., Adkins, J.F., Fernandez, D.P., Burnett, D.S., Wang, S.-L., Gagnon, A.C., Krakauer, N., 2006. Primary  
728 U distribution in scleractinian corals and its implications for U series dating. *Geochem. Geophys. Geosyst.* 7,  
729 Q05022, doi, 10.1029/2005GC001138.
- 730 Rogerson, M., Rohling, E.J., Weaver, P.P.E., Murray, J.W., 2004. The Azores Front since the Last Glacial  
731 Maximum. *Earth Planet. Sci. Lett.* 222, 779-789.
- 732 Rogerson, M., Rohling, E.J., Weaver, P.P.E., Murray, J.W., 2005. Glacial to interglacial changes in the settling  
733 depth of the Mediterranean Outflow plume. *Paleoceanography* 20, PA3007, doi:3010.1029/2004PA001106.
- 734 Rüggeberg, A., Dullo, W.-C., Dorschel, B., Hebbeln, D., 2007. Environmental changes and growth history of a  
735 cold-water carbonate mound (Propeller Mound, Porcupine Seabight). *Int. J. Earth Sci.* 96, 57-72.
- 736 Salgueiro, E., Voelker, A., Abrantes, F., Meggers, H., Pflaumann, U., Loncaric, N., González-Álvarez, R., Oliveira,  
737 P., Bartels-Jónsdóttir, H.B., Moreno, J., Wefer, G., 2008. Planktonic foraminifera from modern sediments reflect  
738 upwelling patterns off Iberia: Insights from a regional transfer function. *Mar. Micropaleontol.* 66, 135-164.
- 739 Sarnthein, M., Tetzlaff, G., Koopmann, B., Wolter, K., Pflaumann, U., 1981. Glacial and interglacial wind regimes  
740 over the eastern tropical Atlantic and Northwest Africa. *Nature* 293, 193-196.
- 741 Schiebel, R., Waniek, J., Bork, M., Hemleben, C., 2001. Planktic foraminiferal production stimulated by  
742 chlorophyll redistribution and entrainment of nutrients. *Deep-Sea Res. I* 48, 721-740.
- 743 Schiebel, R., Waniek, J., Zeltner, A., Alves, M., 2002. Impact of the Azores Front on the distribution of planktic  
744 foraminifers, shelled gastropods and coccolithophorids. *Deep-Sea Res. II* 49, 4035-4050.
- 745 Schmiedl, G., de Bovée, F., Buscail, R., Charrière, B., Hemleben, C., Medernach, L., Picon, P., 2000. Trophic control  
746 of benthic foraminiferal abundance and microhabitat in the bathyal Gulf of Lions, western Mediterranean Sea.  
747 *Mar. Micropaleontol.* 40, 167-188.
- 748 Scholz, D., Mangini, A., Felis, T., 2004. U-series dating of diagenetically altered fossil reef corals. *Earth Planet. Sci.*  
749 *Lett.* 218, 163-178.
- 750 Schönfeld, J., Zahn, R., 2000. Late Glacial to Holocene history of the Mediterranean Outflow. Evidence from  
751 benthic foraminiferal assemblages and stable isotopes at the Portuguese margin. *Palaeogeogr. Palaeoclimat.*  
752 *Palaeoecol.* 159, 85-111.
- 753 Schröder-Ritzrau, A., Freiwald, A., Mangini, A., 2005. U/Th-dating of deep-water corals from the eastern North  
754 Atlantic and the western Mediterranean Sea. In: Freiwald, A., Roberts, J.M. (Eds.), *Cold-water Corals and*  
755 *Ecosystems*. Springer, Heidelberg, pp. 691-700.
- 756 Sierro, F.J., Flores, J.A., Baraza, J., 1999. Late glacial to recent paleoenvironmental changes in the Gulf of Cadiz  
757 and formation of sandy contourite layers. *Mar. Geol.* 155, 157-172.
- 758 Somoza, L., Diaz-del-Rio, V., Leon, R., Ivanov, M., Fernandez-Puga, M.C., Gardner, J.M., Hernandez-Molina, F.J.,  
759 Pinheiro, L.M., Rodero, J., Lobato, A., 2003. Seabed morphology and hydrocarbon seepage in the Gulf of Cádiz  
760 mud volcano area: Acoustic imagery, multibeam and ultra-high resolution seismic data. *Mar. Geol.* 195, 153-  
761 176.
- 762 Stirling, C.H., Esat, T.M., Lambeck, K., McCulloch, M.T., 1998. Timing and duration of the Last Interglacial:  
763 evidence for a restricted interval of widespread coral reef growth. *Earth Planet. Sci. Lett.* 160, 745-762.
- 764 Stoll, H.M., Arevalos, A., Burke, A., Ziveri, P., Mortyn, G., Shimizu, N., Unger, D., 2007. Seasonal cycles in biogenic  
765 production and export in Northern Bay of Bengal sediment traps. *Deep-Sea Res. II* 54, 558-580.

766 Stuut, J.-B.W., Prins, M.A., Schneider, R.R., Weltje, G.J., Jansen, J.H.F., Postma, G., 2002. A 300-kyr record of  
767 aridity and wind strength in southwestern Africa: inferences from grain-size distributions of sediments on  
768 Walvis Ridge, SE Atlantic. *Mar. Geol.* 180, 221-233.

769 Stuut, J.B., Zabel, M., Ratmeyer, V.H., P., Schefuß, E., Lavik, G., Schneider, R.R., 2005. Provenance of present-day  
770 eolian dust collected off NW Africa: implications for deep-marine sediment studies. *J. Geophys. Res.* 110,  
771 D04202.

772 Taviani, M., Bouchet, P., Metivier, B., Fontugne, M., Delibrias, G., 1991. Intermediate steps of southwards faunal  
773 shifts testified by last glacial submerged thanatocoenoses in the Atlantic Ocean. *Palaeogeography,*  
774 *Palaeoclimatology, Palaeoecology* 86, 331-338.

775 Taviani, M., Remia, A., Corselli, C., Freiwald, A., Malinverno, E., Mastrototaro, F., Savini, A., Tursi, A., 2005. First  
776 geo-marine survey of living cold-water *Lophelia* reefs in the Ionian Sea (Mediterranean basin). *Facies* 50, 409-  
777 417.

778 Thiel, H., Pfannkuche, O., Schriever, G., Lochte, K., Gooday, A.J., Hemleben, C., Mantoura, R.F.C., Turley, C.M.,  
779 Patching, J.W., Riemann, F., 1989. Phytodetritus on the deep-sea floor in a central region of the Northeast  
780 Atlantic. *Biol. Oceanogr.* 6, 203-239.

781 Thompson, W.G., Spiegelman, M.W., Goldstein, S.L., Speed, R.C., 2003. An open-system model for U-series age  
782 determinations of fossil corals. *Earth Planet. Sci. Lett.* 210, 365-381.

783 Thunell, R., Reynolds, L., 1984. Sedimentation of planktonic foraminifera: Seasonal changes in species flux in the  
784 Panama Basin. *Micropaleontology* 30, 243-262.

785 Tyler, B., Amaro, T., Arzola, R., Cunha, M.R., De Stigter, H., Gooday, A., Huvenne, V., Ingels, J., Kiriakoulakis, K.,  
786 Lastras, G., Masson, D.G., Oliveira, A., Pattenden, A., Vanreusel, A., Van Weering, T.C.E., Vitorino, J., Witte, U.,  
787 Wolff, G., 2009. Europe's Grand Canyon: Nazaré Submarine Canyon. *Oceanography* 22, 46-57.

788 Tyler, P.A., Harvey, R., Giles, L.A., Gage, J.D., 1992. Reproductive strategies and diet in deep-sea nuculanid  
789 protobranchs (*Bivalvia: Nuculoidea*) from the Rockall Trough. *Mar. Biol.* 114, 571-580.

790 Voelker, A.H.L., Lebreiro, S.M., Schönfeld, J., Cacho, I., Erlenkeuser, H., Abrantes, F., 2006. Mediterranean  
791 outflow strengthening during northern hemisphere coolings: A salt source for the glacial Atlantic. *Earth Planet.*  
792 *Sci. Lett.* 245, 39-55.

793 Waller, R.G., Tyler, P.A., 2005. The reproductive biology of two deep-water, reef-building scleractinians from the  
794 NE Atlantic Ocean. *Coral Reefs* 24, 514-522.

795 Weltje, G., 1997. End-member modeling of compositional data: Numerical-statistical algorithms for solving the  
796 explicit mixing problem. *Math. Geol.* 29, 503-549.

797 Wheeler, A.J., Beyer, A., Freiwald, A., de Haas, H., Huvenne, V., Kozachenko, M., Olu-Le Roy, K., Opderbecke, J.,  
798 2007. Morphology and environment of cold-water coral carbonate mounds on the NW European margin. *Int. J.*  
799 *Earth Sci.* 96, 37-56.

800 White, M., Mohn, C., de Stigter, H., Mottram, G., 2005. Deep-water coral development as a function of  
801 hydrodynamics and surface productivity around the submarine banks of the Rockall Trough, NE Atlantic. In:  
802 Freiwald, A., Roberts, J.M. (Eds.), *Cold-Water Corals and Ecosystems*. Springer, Heidelberg, pp. 503-514.

803 White, M., Roberts, J.M., van Weering, T.C.E., 2007. Do bottom-intensified diurnal tidal currents shape the  
804 alignment of carbonate mounds in the NE Atlantic? *Geo-Mar. Lett.* 27, 391-397.

805 Wienberg, C., Hebbeln, D., Fink, H.G., Mienis, F., Dorschel, B., Vertino, A., López Correa, M., Freiwald, A., 2009.  
806 Scleractinian cold-water corals in the Gulf of Cádiz - first clues about their spatial and temporal distribution.  
807 *Deep-Sea Res. I* 56, 1873-1893.

808 Wilke, I., Meggers, H., Bickert, T., 2009. Depth habitats and seasonal distributions of recent planktic foraminifers  
809 in the Canary Islands region (29°N) based on oxygen isotopes. *Deep-Sea Res. I* 56, 89-106.

810  
811  
812

813 **Figure 1. Map of the Gulf of Cádiz (GoC) showing the coring sites** (bathymetric data source:  
814 GEBCO). Reference sediment core GeoB 9064 (black triangle) and coral-bearing sediment  
815 cores (A-D). A: Hespérides mud volcano (GeoB 9018), B: Faro mud volcano (GeoB 9031, GeoB  
816 9032), C: Renard Ridge (GeoB 9070, GeoB 12101, GeoB 12102, GeoB 12103, GeoB 12104,  
817 M2004-02), D: north of Meknes mud volcano (GeoB 12106). Indicated are the reported  
818 occurrences of fossil cold-water corals (after Wienberg et al., 2009). Lower left: photographs  
819 showing characteristic 'coral graveyards' in the southern GoC, Moroccan margin (position is  
820 indicated on the map as p1, p2) (images ©MARUM, Bremen).

821

822 **Figure 2. Initial U-isotopic ratios of cold-water corals (lower graph) and  $^{232}\text{Th}$  concentration**  
823 **(upper graph).**  $\delta^{234}\text{U}$  is in almost all cases very close to present-day seawater (149.9‰: blue  
824 dashed line; range of  $149.9\pm 10\%$ ‰: light blue bar), except for the deepest sample in core GeoB  
825 12104 (+38‰).  $^{232}\text{Th}$  concentrations for 75% of all samples are below  $10\text{ ng g}^{-1}$  (green dashed  
826 line).

827 **Figure 3.  $^{230}\text{Th}/\text{U}$  datings conducted on cold-water coral fragments collected in the GoC.**  
828 AMS  $^{14}\text{C}$  ages presented by Wienberg et al. (2009) are implemented. Note that solely reef-  
829 forming species such as *Madrepora oculata* and *Lophelia pertusa* are considered showing  
830 that >90% of all coral ages coincide with glacial periods. Marine Isotope Stages (MIS) are  
831 indicated by grey bars based on SPECMAP  $\delta^{18}\text{O}$  stack (Imbrie et al. 1989).

832

833 **Figure 4. Multi-proxy data of sediment core GeoB 9064.** (a) Estimated sedimentation rate,  
834 (b) stable oxygen isotopes record (lower curve) compared with the GRIP ice core record  
835 (upper curve) (c) median grain size (terrigenous and bulk sediment), (d) relative aeolian  
836 input, (e) relative wind strength, and (f) productivity index based on the ratio of high- to  
837 low-productivity planktonic foraminiferal assemblages. AMS  $^{14}\text{C}$  dates obtained for core  
838 GeoB 9064 are marked by black diamonds. For comparison, U/Th (squares; this study) and  
839 AMS  $^{14}\text{C}$  coral dates (triangles; Wienberg et al., 2009) obtained for the past 50 kyr are

840 implemented. Note that solely reef-forming species such as *Madrepora oculata* and  
841 *Lophelia pertusa* are considered.

842

843 **Figure 5. The  $\delta^{18}\text{O}$  record and planktonic foraminiferal abundance for sediment core GeoB**  
844 **9064. (a)  $\delta^{18}\text{O}_{N. pachyderma}$  (dex.), (b) *Neogloboquadrina pachyderma* (black: dex., grey: sin.), (c)**  
845 ***Globigerinita glutinata*, (d) *Globigerina bulloides*, (e) *Globigerinoides ruber* (black) and**  
846 ***Globigerinoides sacculifer* (grey), (f) *Globorotalia inflata*, (g) *Globorotalia scitula*. Younger**  
847 **Dryas (YD) and Marine Isotope Stages (MIS) 2 and 3 are indicated.**

848

849

Figure1

[Click here to download high resolution image](#)

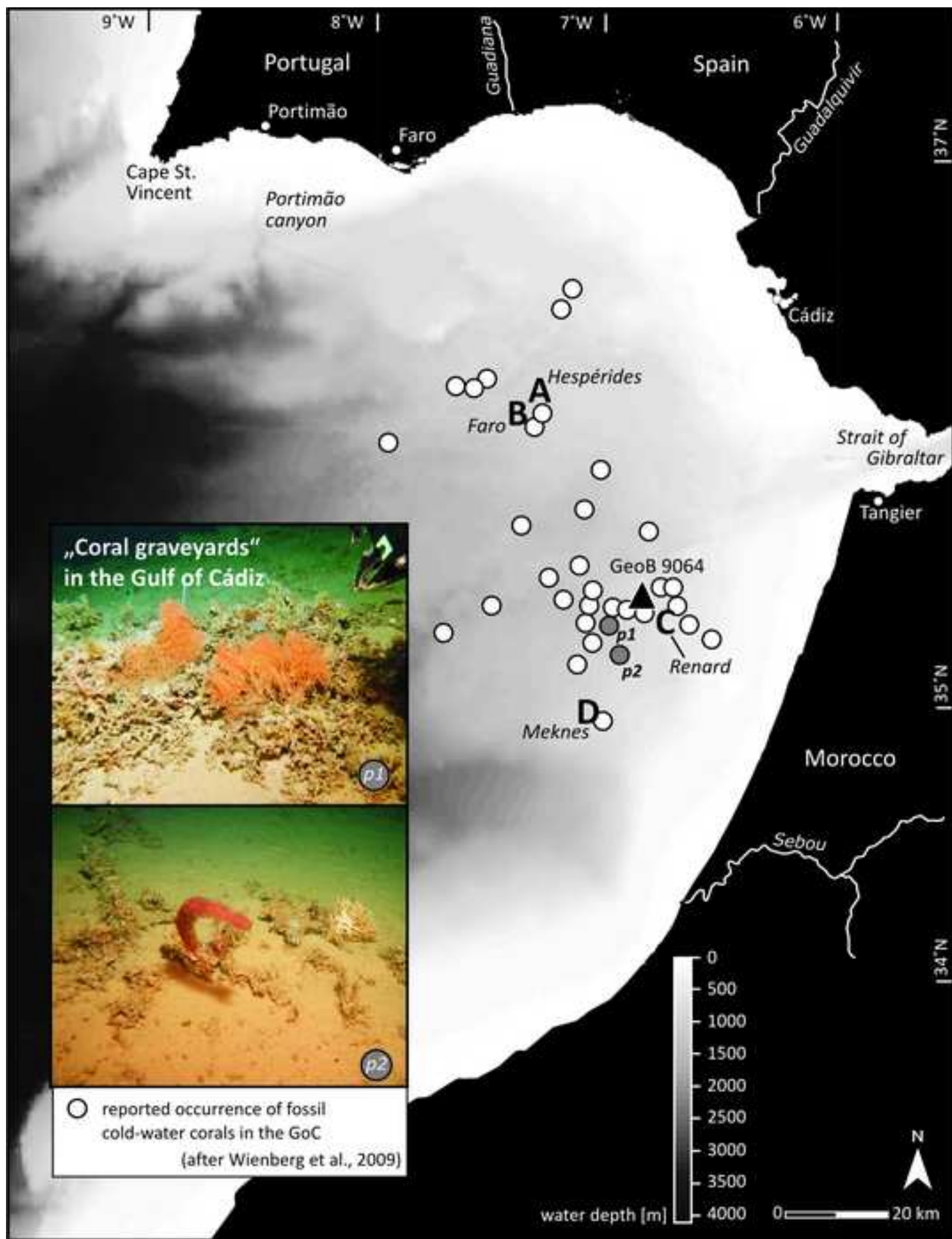


Figure2  
[Click here to download high resolution image](#)

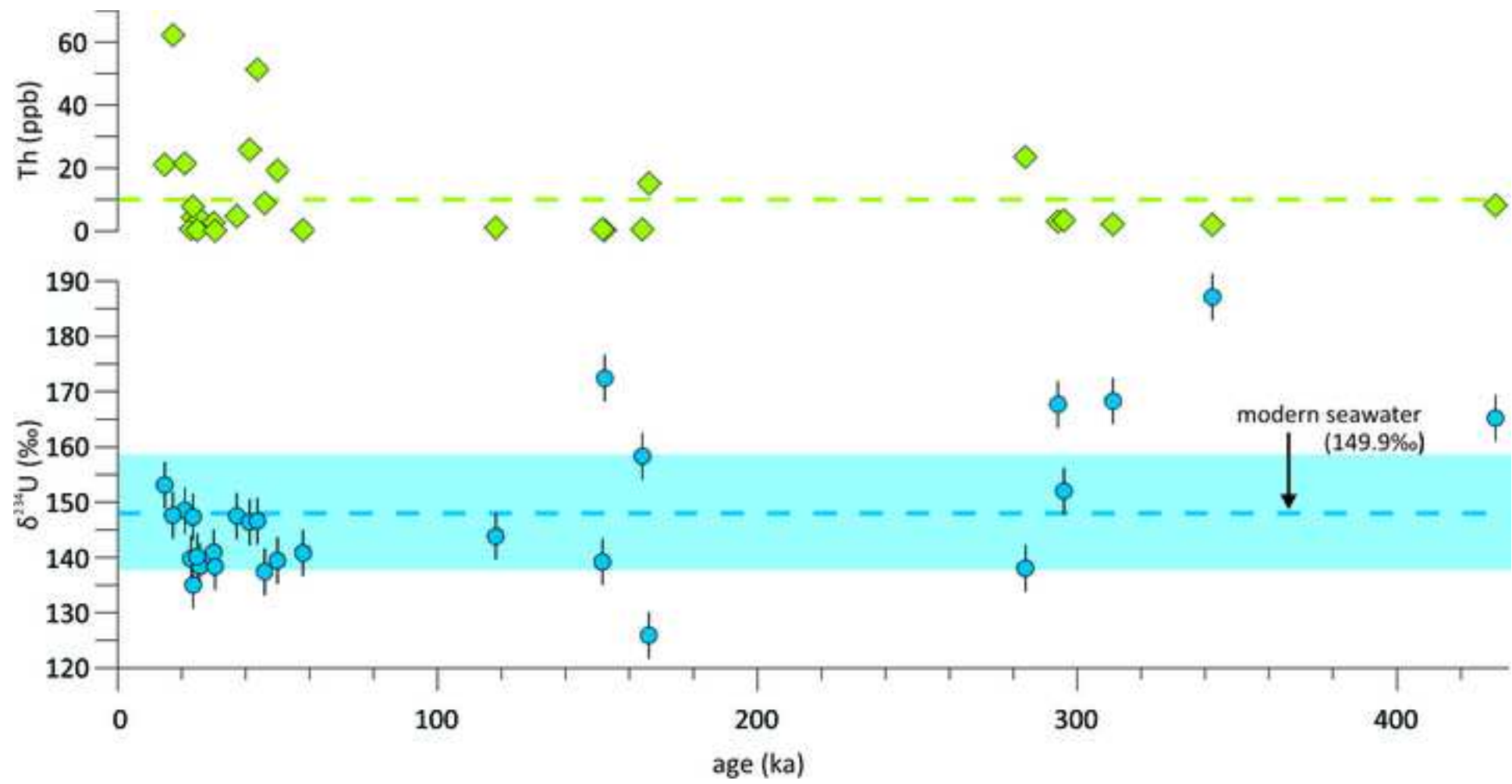


Figure3

[Click here to download high resolution image](#)

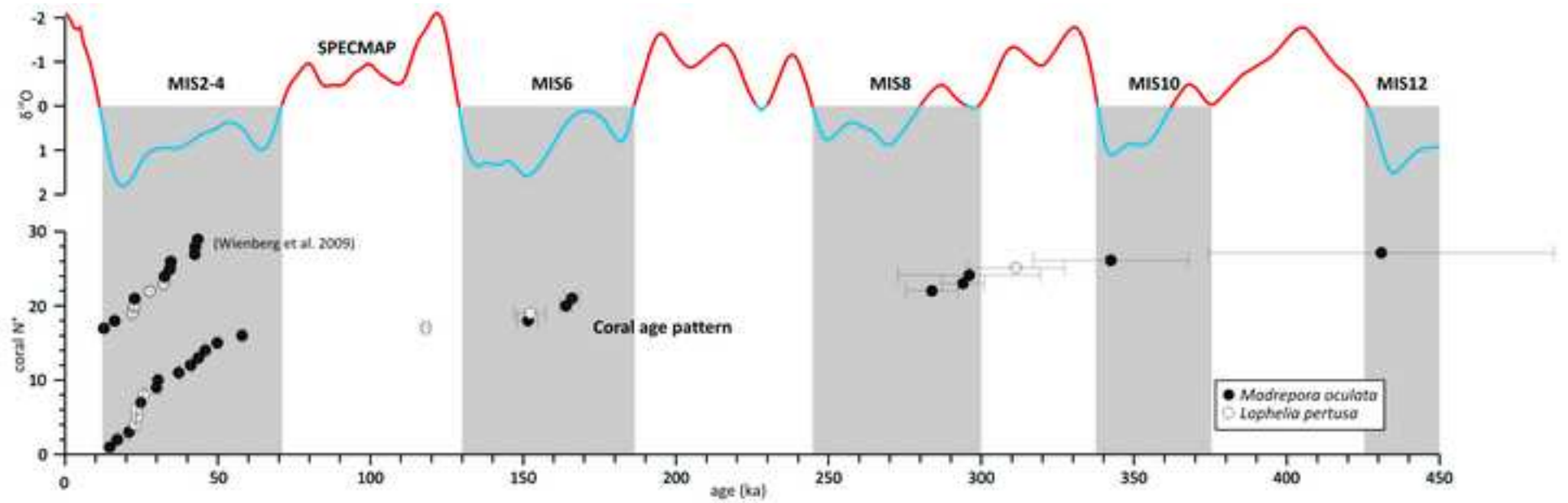




Figure 4

[Click here to download high resolution image](#)

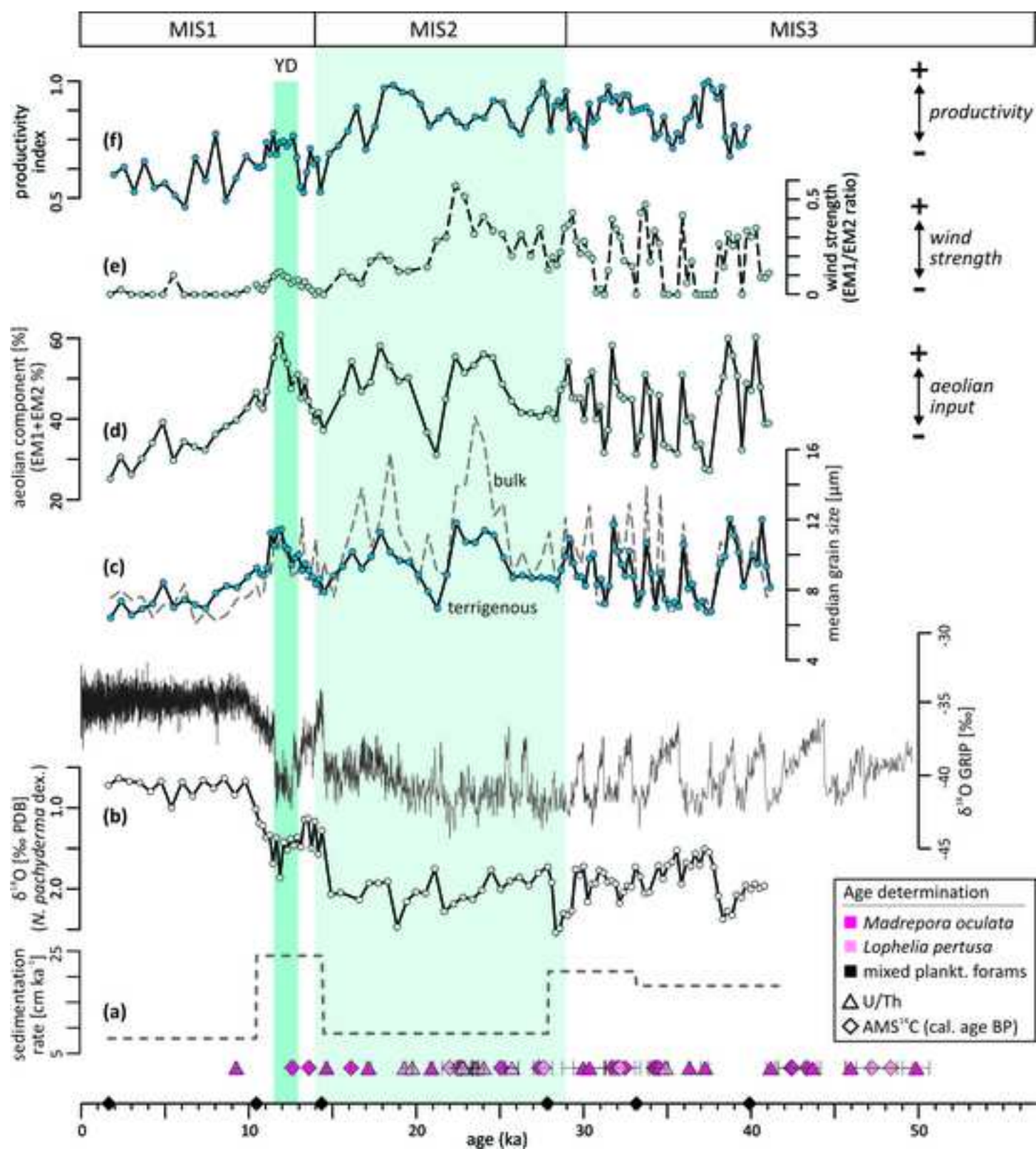
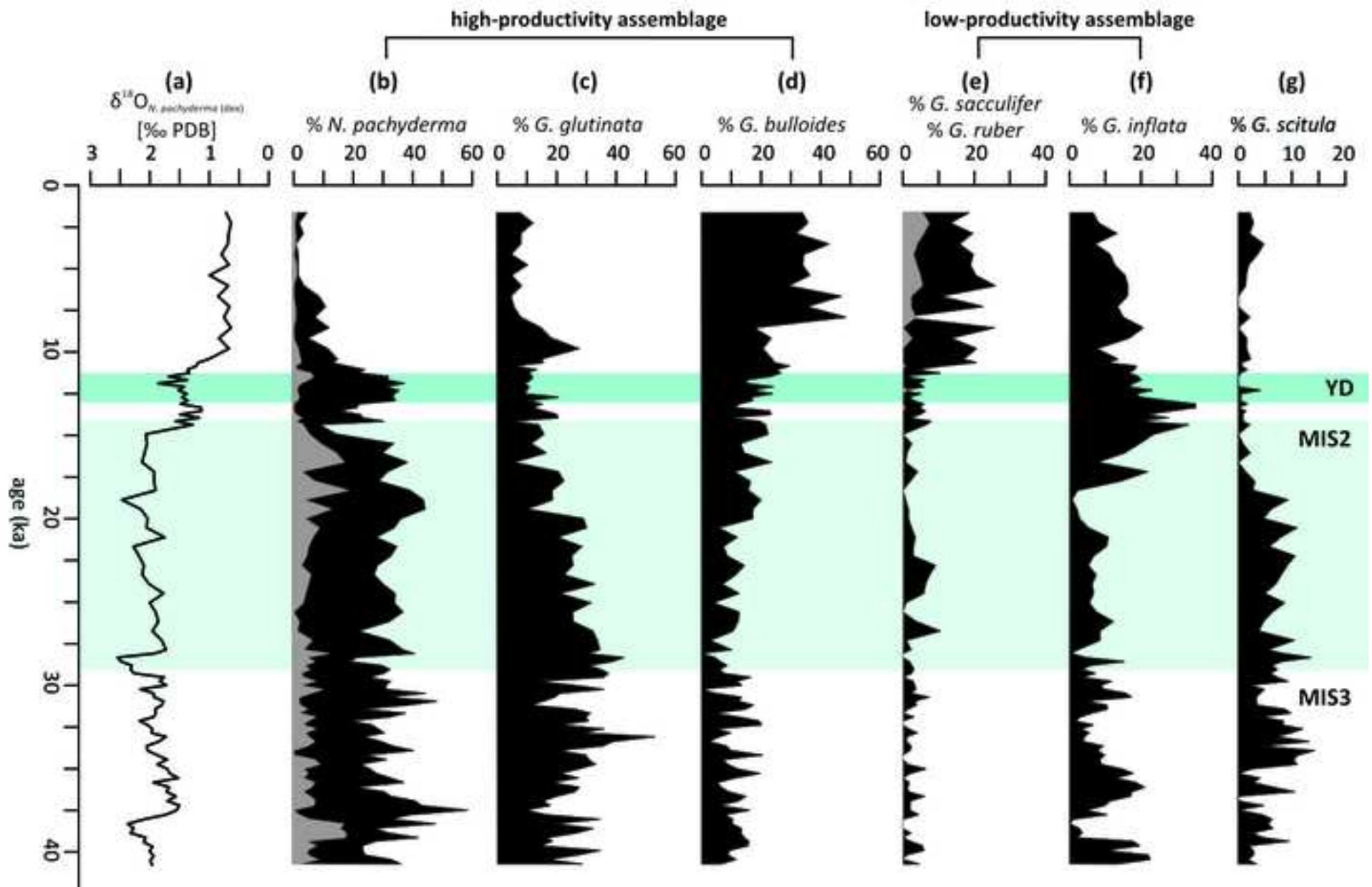


Figure5

[Click here to download high resolution image](#)



1 **Table 1.** Metadata of coral-bearing sediment cores collected from various sites in the Gulf of  
 2 Cádiz (indicated in Figure 1 as A, B, C, D). Abbreviations: Lat, latitude; Lon, longitude; Wd,  
 3 water depth; Rec, recovery; Mv, mud volcano; Cm, coral mound; SM, Spanish margin; MM,  
 4 Moroccan margin; R, Ridge; PDE, Pen Duick Escarpment; Mo, *Madrepora oculata*; Lp, *Lophelia*  
 5 *pertusa*. Cruises: 1, RV *Sonne* cruise SO175; 2, RV *Maria S. Merian* MSM01-3; 3, RV *Pelagia*  
 6 cruise 64PE229.

			Cruise	Location	Core-ID	Lat (°N)	Lon (°W)	Wd (m)	Rec (cm)	Coral content
<b>A</b>	Mv	SM	1	Hespérides Mv	GeoB 9018	36°10.98'	07°18.37'	702	347	0-5 cm: dendrophylliids, 5-347 cm: solely Mo; strongly altered fragments.
<b>B</b>	Mv	SM	1	Faro Mv (lower flank)	GeoB 9031	36°05.75'	07°23.28'	897	484	0-160 cm: Mo-dominated; strongly altered fragments.
	Mv	SM	1	Faro Mv (top)	GeoB 9032	36°05.55'	07°23.57'	843	220	0-60 cm: Mo-dominated, 60-220 cm: mud breccia.
<b>C</b>	Cm	MM	1	W Renard R	GeoB 9070	35°22.00'	06°51.90'	594	560*	0-560 cm: Mo and Lp.
	Cm	MM	2	W Renard R	GeoB 12104	35°21.99'	06°51.90'	590	523	0-523 cm: Mo and Lp
	Cm	MM	2	Renard R	GeoB 12102	35°21.11'	06°50.96'	585	518	0-518 cm: Mo, Lp, and dendrophylliids.
	Cm	MM	2	Renard R	GeoB 12103	35°21.18'	06°50.90'	591	568	0-568 cm: Mo and Lp.
	Cm	MM	2	PDE	GeoB 12101	35°18.88'	06°48.08'	545	468	0-468 cm: Mo, Lp, and dendrophylliids.
	Cm	MM	3	PDE	M2004-02	35°17.68'	06°47.25'	523	861	0-861 cm: Mo, Lp, and dendrophylliids.
<b>D</b>	Cm	MM	2	N of Meknes Mv	GeoB 12106	34°59.49'	07°04.56'	758	303	30-303 cm: Mo and Lp.

7 \* the uppermost 40 cm of core GeoB 9070 were disturbed due to coring operation, thus the undisturbed core  
 8 depth ranges from 40 to 600 cm  
 9

10 **Table 2.** Ages, isotope concentrations and ratios (n.a., not available).

N°	Sample ID	Depth (cm)	Coral	Labcode	Age ± (ka) (ka)	<sup>238</sup> U ± (ppm) (ppm)	<sup>232</sup> Th ± (ppb) (ppb)	$\delta^{234}\text{U(M)}$ ± (‰) (‰)	$\delta^{234}\text{U(0)}$ ± (‰) (‰)
	1	2	3	4	5	6	7	8	9
01	GeoB 9018	3	Mo	n.a.	14.65 0.09	4.020 0.004	21.019 0.052	149.8 1.9	156.1 2.0
02	GeoB 9018	123	Mo	n.a.	294.00 7.00	4.329 0.004	3.021 0.006	73.1 1.4	167.7 3.3
03	GeoB 9018	272	Mo	n.a.	283.80 8.50	4.005 0.004	23.536 0.064	61.9 1.5	138.0 3.3
04	GeoB 9031	10	Mo	n.a.	20.92 0.12	4.956 0.005	21.400 0.055	139.9 1.8	148.5 1.9
05	GeoB 9031	93	Mo	n.a.	37.25 0.23	5.263 0.007	4.796 0.009	132.8 2.3	147.5 2.5
06	GeoB 9031	150	Mo	n.a.	45.94 0.33	4.338 0.004	8.875 0.016	120.6 1.4	137.4 1.6
07	GeoB 9032	20	Mo	n.a.	17.15 0.15	4.447 0.005	62.092 0.192	140.6 1.6	147.6 1.7
08	GeoB 9032	47	Mo	n.a.	41.17 0.25	4.512 0.005	25.841 0.070	130.3 1.8	146.4 2.0
09	GeoB 9070	47	Lp	n.a.	23.50 0.12	4.622 0.003	4.428 0.010	137.9 1.1	147.3 1.2
10	GeoB 9070	298	Mo	n.a.	43.68 0.28	3.552 0.003	51.216 0.079	129.6 1.8	146.6 2.0
11	GeoB 9070	520	Mo	n.a.	166.00 2.40	3.968 0.004	15.089 0.033	78.7 1.7	125.9 2.7
12	GeoB 12101	57	Mo	Gif-1525	<i>not dateable</i>	3.085 0.004	0.351 0.002	59.5 3.2	/ /
13	GeoB 12101	146	Lp	Gif-1389	<i>not dateable</i>	3.214 0.004	0.920 0.003	47.4 3.0	/ /
14	GeoB 12101	451	Mo	Gif-1527	430.76 56.55	2.589 0.002	8.092 0.026	48.9 3.3	165.2 3.3
15	GeoB 12102	28	Mo	Gif-1529	57.96 0.74	4.390 0.005	0.316 0.001	119.5 2.7	140.8 2.7
16	GeoB 12102	166	Lp	Gif-1528	118.16 1.10	4.220 0.003	1.075 0.003	103.0 1.9	143.8 1.9
17	GeoB 12102	238	Lp	Gif-1390	152.27 5.12	3.035 0.003	0.306 0.003	112.1 2.9	172.4 2.9
18	GeoB 12102	376	Mo	Gif-1388	151.56 3.37	3.614 0.003	0.491 0.002	90.7 3.0	139.2 3.0
19	GeoB 12102	493	Mo	Gif-1386	164.02 2.01	3.194 0.003	0.495 0.002	99.5 1.8	158.3 1.8
20	GeoB 12103	34	Lp	Gif-1530	22.88 0.38	3.881 0.004	0.636 0.003	131.0 2.0	139.8 2.0
21	GeoB 12103	88	Lp	Gif-1392	25.72 0.39	4.462 0.006	3.873 0.010	128.7 2.9	138.4 2.9
22	GeoB 12103	200	Mo	Gif-1531	29.98 1.26	3.610 0.004	2.644 0.011	129.4 3.3	140.9 3.3
23	GeoB 12103	317	Mo	Gif-1532	30.43 0.96	3.828 0.004	0.192 0.003	126.9 2.2	138.3 2.2
24	GeoB 12103	444	Mo	Gif-1533	49.85 0.80	3.693 0.005	19.205 0.071	121.1 2.4	139.4 2.4
25	GeoB 12104	8	Lp	Gif-1387	23.57 0.18	4.435 0.003	7.778 0.016	126.3 1.7	135.0 1.7
26	GeoB 12104	373	Lp	Gif-1534	311.20 15.74	3.658 0.003	2.161 0.012	69.8 2.2	168.3 2.2
27	GeoB 12104	491	Mo	Gif-1535	342.29 25.38	3.492 0.004	2.003 0.008	71.1 2.6	187.1 2.6
28	GeoB 12106	117	Mo	Gif-1391	295.86 23.27	3.421 0.004	3.421 0.004	65.9 2.8	152.0 2.8
29	M2004-02	49	Mo	Gif-1631	9.15 0.71	3.512 0.011	0.103 0.014	149.3 3.0	153.2 3.0
30	M2004-02	85	Lp	Gif-1632	19.36 0.54	3.943 0.007	0.625 0.008	138.8 2.5	146.6 2.5
31	M2004-02	105	Lp	Gif-1633	19.87 0.52	3.284 0.010	0.695 0.006	136.0 3.9	143.9 3.9
32	M2004-02	141	Lp	Gif-1634	21.37 0.42	3.862 0.007	4.666 0.013	136.5 2.3	145.0 2.3
33	M2004-02	147	Lp	Gif-1635	22.75 0.26	4.016 0.006	2.209 0.006	133.0 2.9	141.8 2.9
34	M2004-02	176	Lp	Gif-1636	24.03 0.26	3.921 0.008	11.534 0.031	131.4 3.3	140.6 3.3
35	M2004-02	247	Lp	Gif-1637	34.90 0.43	3.099 0.004	0.310 0.001	130.3 2.5	143.8 2.5
36	M2004-02	273	Mo	Gif-1638	36.27 0.43	3.804 0.008	3.049 0.008	124.5 1.6	138.0 1.6
37	M2004-02	313	Lp	Gif-1639	142.08 1.92	4.068 0.010	2.908 0.009	96.6 2.3	144.4 2.4
38	M2004-02	343	Lp	Gif-1640	175.01 2.79	3.846 0.005	14.820 0.026	85.3 2.5	139.9 2.5
39	M2004-02	363	Mo	Gif-1641	242.07 8.35	3.174 0.008	0.506 0.003	85.4 2.7	169.3 2.7
40	M2004-02	403	Lp	Gif-1642	262.80 7.46	3.126 0.007	3.116 0.007	74.2 2.9	155.9 2.9

11 **NOTE:** **Column 1:** Sample label. **Column 2:** Depth in core. **Column 3:** Reef-forming scleractinian cold-water coral species, Lp  
12 *Lophelia pertusa*, Mo *Madrepora oculata*. **Column 4:** Labcode (not available for datings conducted at IFM-GEOMAR, N° 1-  
13 11). **Column 5:** Calculated coral ages. **Column 6:** <sup>238</sup>U concentration. **Column 7:** <sup>232</sup>Th concentration. **Column 8:** Measured  
14 <sup>234</sup>U/<sup>238</sup>U activity ratios ( $\delta^{234}\text{U(M)}$ ) are presented as deviation per mil (‰) from the equilibrium value. **Column 9:** Decay  
15 corrected <sup>234</sup>U/<sup>238</sup>U activity ratios ( $\delta^{234}\text{U(0)}$ ) are calculated from the given ages and with  $\lambda_{234\text{U}} = 2.8263 \times 10^{-6} \text{ yr}^{-1}$ . Note that  
16 ages are strictly reliable having values between 146.6‰ and 149.6‰ (modern seawater), reliable with values of 149±10‰,  
17 unreliable with values >149±10‰ (see also Stirling et al., 1998; Robinson et al., 2004; Esat and Yokoyama, 2006).  
18

19 **Table 3.** AMS <sup>14</sup>C dates determined on multi-species samples of planktonic foraminifera  
 20 from sediment core GeoB 9064. The AMS <sup>14</sup>C ages were corrected for <sup>13</sup>C and a mean ocean  
 21 reservoir age of 400 years, and were converted to calendar years using the CALPAL 2007  
 22 Hulu software. Estimated sedimentation rates for core GeoB 9064 are supplemented.

Core depth (cm)	Labcode	Conventional age		CALPAL age		Sedimentation rate (cm kyr <sup>-1</sup> )
		<sup>14</sup> C age (years)	± error	1σ (68%) (calendar years B.P., P.=AD 1950)	± error	
<b>GeoB 9064</b>						
4	Poz-20282	2 095	30	1 630	50	-
74	KIA-10065	9 665	60	10 430	100	7.95
169	KIA-13060	12 660	80	14 370	240	24.11
289	KIA-23840	23 440	180	27 860	190	8.90
399	KIA-29420	29 020	320	33 090	420	21.03
524	KIA-35660	35 260	630	39 960	960	18.20

23